https://doi.org/10.5194/egusphere-2025-3517
Preprint. Discussion started: 10 September 2025

Benchmarking soil moisture and its relationship to ecohydrologic variables in Earth System Models

Elias C. Massoud[1], Nathan Collier[1], Yaoping Wang[1], Jiafu Mao[1], Adrian Harpold[2], Steven A. Kannenberg[3], Gerbrand Koren[4], Mukesh Kumar[5], Pushpendra Raghav[5], Pallav Ray[6], Mingjie Shi[7], Jing Tao[8], Sreedevi P. Vasu[6], Huiqi Wang[9], Qing Zhu[8], Forrest M. Hoffman[1]

[1] Oak Ridge National Laboratory, Oak Ridge, TN 37830, USA
[2] University of Nevada, Reno, Reno, NV 89557, USA
[3] Department of Biology, West Virginia University, Morgantown, WV 26506, USA
[4] Copernicus Institute of Sustainable Development, Utrecht University, Princetonlaan 8a, 3584 CB Utrecht, Netherlands
[5] Department of Civil, Construction, and Environmental Engineering, University of Alabama, Tuscaloosa, AL 35487, USA
[6] Florida Institute of Technology, Melbourne, FL 32901, USA
[7] Pacific Northwest National Laboratory, Richland, WA 99352, USA
[8] Lawrence Berkeley National Laboratory, Berkeley, CA 94720, USA
[9] University of California, Berkeley, Berkeley, CA 94720, USA

Correspondence to: Elias C. Massoud (massoudec@ornl.gov)

Abstract. Soil moisture (SM) is a key regulator of ecosystem biogeophysics, influencing plant water relations and land-atmosphere energy exchanges. This study evaluates the representation of SM in Earth System Models (ESMs) using the International Land Model Benchmarking (ILAMB) framework, focusing on both surface (0–5 cm, 0–10 cm) and rootzone (0–100 cm) depths. We benchmark Coupled Model Intercomparison Project Phase 6 (CMIP6) models against multiple observational and assimilated datasets to evaluate their performance in simulating SM, as well as their relationships with ecohydrological processes and vegetation traits such as gross primary productivity (GPP), leaf area index (LAI), and evapotranspiration (ET). Results show that while surface SM is generally well represented ($r > 0.87$), rootzone SM variability is overestimated (normalized standard deviation > 1). Simulated ET agrees strongly with observations ($r > 0.9$; normalized standard deviation 0.8-1.2), whereas GPP and LAI exhibit greater discrepancies ($r > 0.7$; normalized standard deviation mostly > 1). The strength of SM–ecohydrology relationships varies with model structure and observational dataset, with better consistency observed when assimilated SM products are used. Regional analyses using Köppen classifications reveal distinct model behaviors, with stronger performance in tropical zones and reduced skill in high-latitude regions, likely due to challenges in simulating freeze–thaw and permafrost dynamics. These findings offer quantitative benchmarks of model performance, highlighting specific areas for improving SM representation and its coupling with vegetation and hydrological processes in future ESM development.

https://doi.org/10.5194/egusphere-2025-3517
Preprint. Discussion started: 10 September 2025

1 Introduction

Soil moisture (SM) plays a central role in regulating Earth system processes by controlling the storage and exchange of water, carbon, and energy between the land surface and atmosphere (Clark et al., 2015; Trugman et al., 2018; Green et al., 2019; Massoud et al., 2020). Accurately representing SM in Earth System Models (ESMs) is essential for improving predictions of the Earth system (Seneviratne et al., 2010; Hauser et al., 2016; Humphrey et al., 2021). ESMs simulate these processes through coupled biogeochemical and hydrological cycles, both of which are strongly influenced by SM. However, accurately modeling SM at ESM grid scales remains challenging due to heterogeneity in soil properties, scale mismatches between physical processes and model resolution, and limited knowledge of subsurface boundary conditions (e.g., groundwater depth). As a result, ESMs adopt a range of approaches to simulate SM, most commonly relying on "bucket-type" models that route water through discrete soil layers using threshold-based parameters (e.g., field capacity) and rate-dependent functions (e.g., hydraulic conductivity). This work seeks to evaluate the representation of SM in ESMs by incorporating the International Land Model Benchmarking (ILAMB) framework (Collier et al., 2018), a tool extensively used to assess the performance of land models. Although ILAMB has been applied to various ecohydrologic processes and properties such as gross primary production (GPP) (Caen et al., 2022), evapotranspiration (ET) (Wu et al., 2020), and leaf area index (LAI) (Yang et al., 2023), SM has remained mostly underrepresented in ILAMB-based model evaluations until now.

Despite advances in ESMs, the accurate simulation of SM in Coupled Model Intercomparison Project Phase 6 (CMIP6) remains a persistent challenge due to structural biases and uncertainties in land surface processes. Several studies have highlighted both improvements and limitations in how CMIP6 models represent SM. For example, Yuan et al. (2021) showed that CMIP6 models better capture historical surface SM trends over the contiguous United States (CONUS) compared to CMIP5, particularly in regions like the Northwest and Midwest. However, considerable inter-model variability remains, suggesting a need for further refinement in future model generations. Similarly, Wang et al. (2022) conducted a comprehensive evaluation of CMIP6 SM simulations over China and found that while the multi-model mean (MME) generally captured observed spatial patterns and seasonal cycles of both near-surface and rootzone SM, substantial inter-model spread persisted, particularly in trends and interannual variability. Their findings also emphasized the dominant role of land surface schemes in driving model behavior, as models developed by the same institution often exhibited similar performance. Moreover, Purdy et al. (2018) illustrated the potential for significant improvement in model performance through better SM representation, showing that integrating SM information from satellite data into model simulations reduced global ET errors by up to 23% in dry regions. These studies point to the critical need to identify and correct structural biases that limit current model skill in simulating SM.

At the same time, the importance of accurately simulating SM extends beyond model performance metrics. Zuo et al. (2024) highlighted that maintaining current global SM levels could reduce nearly a third of projected land warming under low-emission scenarios. Their results, based on outputs from historical CMIP6 experiments and other model intercomparison projects, highlight the central role SM plays in climate feedbacks and the reliance on models like CMIP6 to inform future projections. Given both the challenges and stakes involved, this study benchmarks SM and its coupling with ecohydrologic processes such as GPP, LAI, and ET, with the goal of identifying model limitations and guiding improvements as we look toward CMIP7 and beyond.

The evaluation of SM in global models has a long history, with early efforts dating back to Robock et al., (1998) as part of the Atmospheric Model Intercomparison Project (AMIP). In their analysis, they found significant discrepancies in how SM was represented and simulated across different models, an issue that was prominent 25 years ago and remains a challenge today. More recently, Qiao et al., (2022) conducted a detailed evaluation of SM using a suite of CMIP6 models, examining both surface and deeper SM (up to 2 meters) across various subregions around the globe. They found that the multimodel ensemble mean generally produces reasonable representations for overall climatology. However, their study relied on

https://doi.org/10.5194/egusphere-2025-3517
Preprint. Discussion started: 10 September 2025

reanalysis products and data assimilation systems as the reference for benchmarking (Qiao et al., 2022), which, while widely used, are not true SM observational products but rather model-based estimates. Furthermore, Qiao et al. (2022) assumed that the model outputs mrsos (surface SM) and mrsol (layered SM) represent the same variable, despite their structural differences (Massoud et al., 2025, in review). In reality, mrsol provides moisture values at multiple soil layers, from which mrsos, representing moisture in the top 10 cm of soil, is derived. Other studies used a combination of observation and model-based benchmarks, but are limited to regional domains and similarly do not distinguish the different nature of mrsos and mrsol (Yuan et al. 2021; Wang et al. 2022). In this current study, we distinguish between these two variables and apply depth-specific derivations to more accurately evaluate SM representation across different layers in the models. Here, we not only benchmark SM at various depths, but also evaluate key ecohydrologic variables such as GPP, LAI, and ET, both individually and in relation to SM, to provide a more comprehensive assessment of land surface processes in CMIP6 models.

One of the persistent challenges in benchmarking SM is the limited availability of high-quality datasets. To address this, we utilize two key datasets for global-scale benchmarking in this study. The first is the Wang et al. (2021) product, which is a weighted average of multiple sources, including offline land surface model simulations, remote sensing data, and reanalysis products, that was found to outperform the original sources in that study. This dataset provides estimates for both surface SM (top 10 cm) and rootzone SM (up to 1 m), offering a view of SM at different depths. The second dataset is the European Space Agency Climate Change Initiative SM (ESA-CCI SM) product (Dorigo et al., 2017; Gruber et al., 2019; Preimesberger et al., 2021), which is derived from a blend of passive and active satellite sensors. ESA-CCI SM represents surface SM down to 5 cm, and its combination of different satellite platforms helps mitigate the limitations of individual sensors, providing an observational estimate for surface SM that is robust. Together, these datasets allow for a more thorough evaluation of SM in CMIP6 models.

While benchmarking SM alone can offer insights into model performance, understanding how SM interacts with other ecosystem processes such as GPP, ET, and LAI can yield additional clues into the strengths and weaknesses of these models (Guswa et al., 2002; Wang et al., 2019). By examining how models' skills are related to certain model processes, we aim to uncover patterns that point to specific model limitations, whether they stem from structural design, input data, or parameterizations. Ultimately, this work seeks to guide improvements in model development and reduce uncertainties in global SM simulations. The goals of this study are threefold. First, we benchmark CMIP6 models in their simulation of SM at multiple depths, specifically at 5 cm, 10 cm, and 100 cm, using various datasets. Second, we assess model performance in simulating key ecohydrologic variables, including GPP, LAI, ET, as well as the relationships between SM and each of these variables. Third, we aim to identify specific areas for improvement, whether in individual models or as systematic issues across the CMIP6 ensemble. To support these objectives, we also implement a Köppen climate region analysis (Geiger 1954) within the ILAMB framework to evaluate model performance across distinct climate zones.

2 Materials and Methods

2.1 Models and Variables in CMIP6 Simulations

The model data used in this study come from CMIP6 (Eyring et al., 2016), an international effort to standardize ESM simulations, enabling direct comparison across models. We use a suite of CMIP6 models (detailed in Table 1) that differ in their spatial resolutions and land surface model components. Table 1 lists each model's horizontal grid spacing and the land surface scheme used to simulate SM, GPP, LAI, and ET.

The SM variables analyzed are mrsol and mrsos, which represent layered and surface soil moisture, respectively. Both variables are provided in units of mass per unit area [kg m^{-2}]. Other simulated variables include gpp (units g m^2 d^{-1}), lai (unitless), and evspsbl (units mm d^{-1}) corresponding to GPP, LAI, and ET. All variables are analyzed at monthly temporal resolution.

https://doi.org/10.5194/egusphere-2025-3517
Preprint. Discussion started: 10 September 2025

To derive SM at specific depths (e.g., 0–5 cm, 0–10 cm, or 0–100 cm), we calculate depth-integrated soil moisture estimates from the mrsol variable, which provides total SM contained in each discrete model soil layer. Since the vertical layering varies across models, we apply a depth-weighted integration approach that also converts units from mass to volumetric SM (i.e., from [kg m^{-2}] to [m^3/m^3]). This conversion and integration is expressed as:

$$SM_{integrated} = \left\{\left[\sum_{layer\ i=1}^{layer\ n-1} \frac{mrsol(i)}{\rho_w * dz(i)} * dz(i)\right] + \left[\frac{mrsol(n)}{\rho_w * dz(i)} * z_{remaining}\right]\right\} \Big/ z_{total} \quad (1)$$

In this equation, $mrsol(i)$ represents the mass of SM in the i-th model-defined soil layer, reported in units of [kg m^{-2}]. The variable ρ_w is the density of liquid water, assumed to be a constant value of 1000 kg/m^3. The quantity $dz(i)$ refers to the thickness of the i-th soil layer in meters [m], which is used to compute the volumetric contribution of each layer. The term $z_{remaining}$ represents the portion in [m] of the final layer that partially overlaps with the target integration depth (e.g., if the target is 10 cm and the final layer spans from 8–15 cm, then $z_{remaining}$=2 cm=0.02 m. The total integration depth, z_{total}, is the sum of all full-layer thicknesses plus $z_{remaining}$, defining the vertical extent over which SM is integrated.

This formula first converts each layer's SM from mass per unit area [kg m^{-2}] to volumetric SM [m3/m3] by dividing by the product of water density and layer thickness. Then, it multiplies by the layer thickness to compute the volume per unit area. Summing over all layers and dividing by the total soil depth yields the average volumetric SM over the target depth. This method standardizes SM across models with differing vertical discretizations and unit conventions, enabling accurate and consistent comparisons with benchmarking datasets, which report SM as a volume fraction. For surface SM (mrsos), which represents a shallow fixed-depth layer (i.e., 0.1 m), we apply the same conversion logic by assuming that fixed depth during volumetric transformation. This approach is consistent with prior studies (e.g., Qiao et al., 2022; Wang et al., 2022; Massoud et al., 2025).

CMIP6 Model Name	Spatial Resolution (~lon° x lat°)	Land Model	Total Soil Depth (m)	# of Soil Layers
ACCESS-ESM1-5	1.875 × 1.25	CABLE	2.87	6
AWI-ESM-1-1-LR	1.875 × 1.875	JSBACH	6.98	5
BCC-ESM1	2.8 × 2.8	BCC-AVIM2	2.86	10
CanESM5-1	2.8 × 2.8	CLASS	4.10	3
CESM2	1.25 × 0.94	CLM5	8.03	20
CMCC-ESM2	1.25 × 0.94	CLM4.5	35.18	15
CNRM-ESM2-1	1.41 × 1.41	ISBA	≤12 m for soil temp; rooting ≤8 m	14
EC-EARTH3-CC	0.70 × 0.70	HTESSEL and LPJ-GUESSv4	1.945	4

https://doi.org/10.5194/egusphere-2025-3517
Preprint. Discussion started: 10 September 2025

GFDL-ESM4	1.0 × 1.0	LM4.1-PPA	8.75	20
GISS-E3-G	2.5 × 2.0	GISS LSM	3.50	6
MPI-ESM1-2-LR	1.875 × 1.875	JSBACH	6.98	5
MRI-ESM2-0	1.125 × 1.125	AGCM	10.0	14
NorESM2-LM	2.5 × 1.875	CLM5	8.03	20
SAM0-UNICON	1.25 × 0.94	CLM4.0	8.03	20
TaiESM1	1.25 × 0.94	CLM4.0	8.03	20
UKESM1-0-LL	1.875 × 1.25	JULES-ES-1.0	3.0	4

Table 1: CMIP6 models used in this study, along with their latitude and longitude grid sizes and the land models with their soil depths and number of soil layers used in each model.

2.2 Soil Moisture Datasets Used for Benchmarking

In this study, we evaluate the SM performance of CMIP6 models using two primary benchmark datasets. The first is the ESA-CCI SM product (Dorigo et al., 2017; Gruber et al., 2019; Preimesberger et al., 2021), which provides a global, long-term record of surface SM (~2-5 cm) spanning over 40 years (1978-2023) at a daily temporal resolution that is aggregate to reflect monthly values and spatial resolution of approximately 25 km (Figure 1A). The ESA-CCI SM product is updated annually through an algorithmic process that incorporates data from both passive and active satellite sensors, producing a blended dataset that integrates multiple sensor sources while extending the time series with each update. This dataset has been extensively used in hydrological and climatological research (e.g., An et al., 2016; McNally et al., 2016; Ciabatta et al., 2018; Massoud et al., 2023; Li et al., 2025a), including the Bulletin of the American Meteorological Society's annual "State of the Climate" reports. Its long-term, global coverage makes it a valuable resource for evaluating surface SM in ESMs. To facilitate direct comparison with the ESA-CCI SM product that typically represents SM at a depth of 5 cm, the mrsol variable in each CMIP6 model is integrated to the 5 cm layer using Eq. 1. Given that some models have first layers that are deeper than 5 cm, this integration may introduce additional uncertainty in the estimated SM.

The second SM dataset used in this study is the Wang et al. (2021) product, which provides a global, gap-free, long-term record of SM across four depths (0–10, 10–30, 30–50, and 50–100 cm) from 1970 to 2016, with a monthly temporal resolution and spatial resolution of 0.5 degrees. This dataset synthesizes SM information from diverse sources, including in situ observations, satellite data, reanalysis products, and offline land surface model simulations. It employs three statistical approaches, unweighted averaging, optimal linear combination (OLC), and emergent constraint (EC), to produce a merged product that outperforms individual source datasets in terms of bias, root mean square error (RMSE), and correlation when compared to in situ observations. For this study, we utilize the OLC version of the Wang et al. (2021) product, which we hereafter refer to as Wang2021OLC, because it is constrained by in situ observational values and performs among the best of the paper's reported method-data source combinations. This hybrid dataset offers harmonized spatial, temporal, and vertical coverage, making it highly suitable for large-scale ESM benchmarking of both surface (Figure 1B) and rootzone (Figure 1C) SM. Since this dataset provides SM estimates at both 10 cm and 100 cm depths, we integrate the mrsol variable from each CMIP6 model to these depths using Eq. 1 to enable direct comparison. In addition, because the mrsos variable in CMIP6 models also represents surface SM at approximately 10 cm, it is separately benchmarked against the 10 cm layer from the Wang2021OLC product. This dual use of mrsol and mrsos allows us to assess the internal consistency and depth

https://doi.org/10.5194/egusphere-2025-3517
Preprint. Discussion started: 10 September 2025

representation of SM across different model variables and observational references.

While these datasets are widely used and provide valuable long-term, global-scale estimates, each has inherent limitations, including retrieval uncertainties, differences in spatial and temporal resolution, and dependence on model-based or algorithmic assumptions. Because no single dataset can fully capture the complexity of SM dynamics, the use of multiple, complementary observational and assimilated products helps quantify uncertainty in the benchmark results presented here.

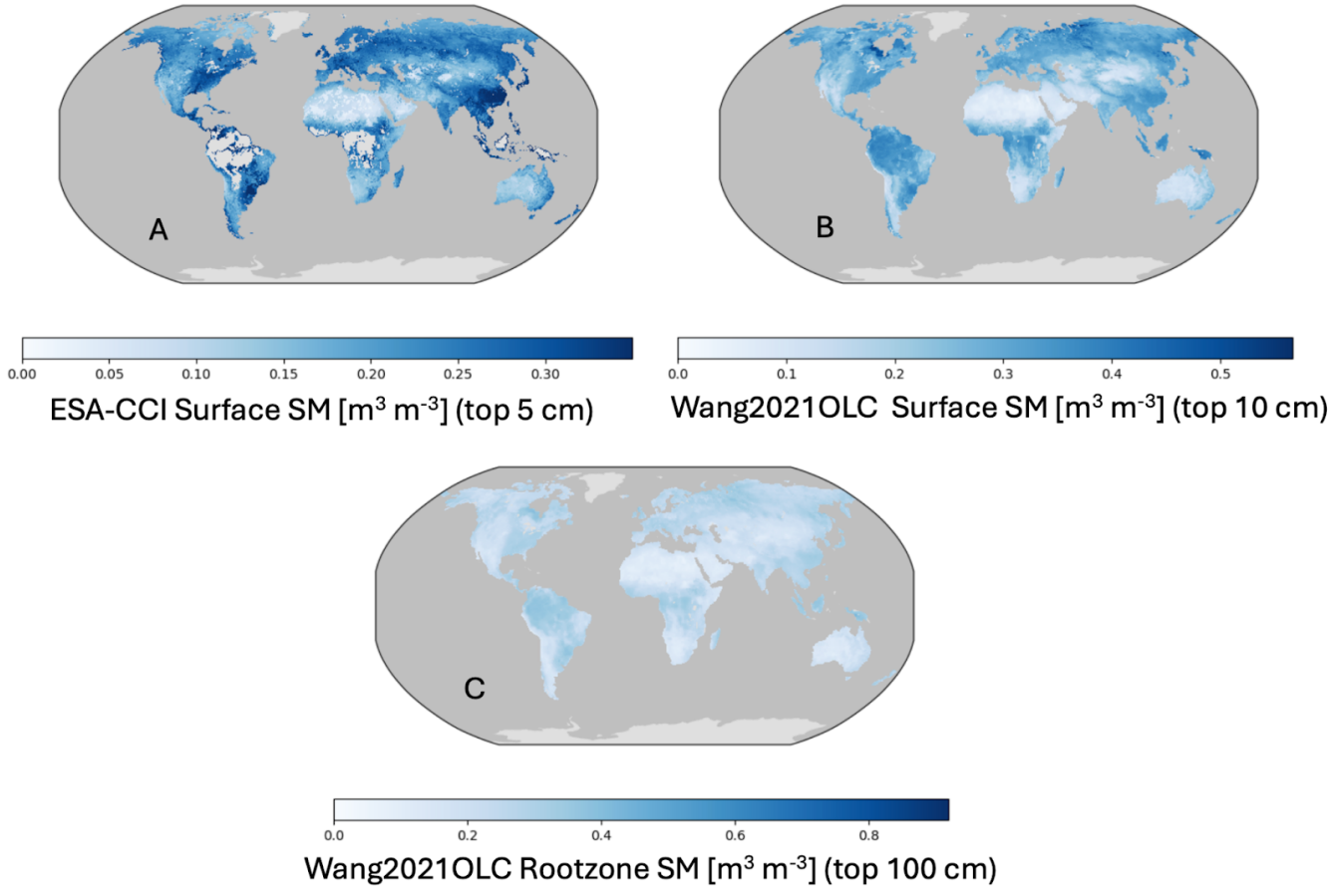

Figure 1: Long-term mean soil moisture (SM) from observational datasets. (A) ESA-CCI Surface SM [m³ m⁻³] (top 5 cm) (1978-2023), providing global estimates based on satellite data. (B) Wang et al. (2021) OLC Surface SM [m³ m⁻³] (top 10 cm) (1970-2016), derived from a merged dataset of satellite and in-situ observations. (C) Wang et al. (2021) OLC Rootzone SM [m³ m⁻³] (top 100 cm), representing long-term mean soil moisture across the rootzone. Each subplot shows the global distribution of soil moisture at the depths represented in each product.

2.3 Other Benchmark Datasets

For the ecohydrologic relationship variables, we incorporate observational datasets specific to each variable that exist in the ILAMB data library. GPP observations are derived from the Water, Energy, and Carbon with Artificial Neural Networks (WECANN) dataset, which provides globally gridded estimates based on advanced machine learning approaches that integrate remote sensing and meteorological inputs (Alemohammad et al., 2017) from 2007 to 2016. LAI data is sourced from the NOAA Climate Data Record (CDR) of AVHRR Leaf Area Index (AVH15C1) from 1981 to 2019 (Claverie et al.,

https://doi.org/10.5194/egusphere-2025-3517
Preprint. Discussion started: 10 September 2025

195 2016). ET data comes from the Global Land Evaporation Amsterdam Model (GLEAM) v3.3a, which provides daily estimates (aggregated here to reflect monthly values) from 1980 to 2018 (Miralles et al., 2011; Martens et al., 2017). The spatial resolution of the WECANN GPP product (Figure 2A) is 0.5°, that of the AVH15C1 LAI data (Figure 2B) is 0.05°, and that of the GLEAMv3.3a ET data (Figure 2C) is 0.25°.

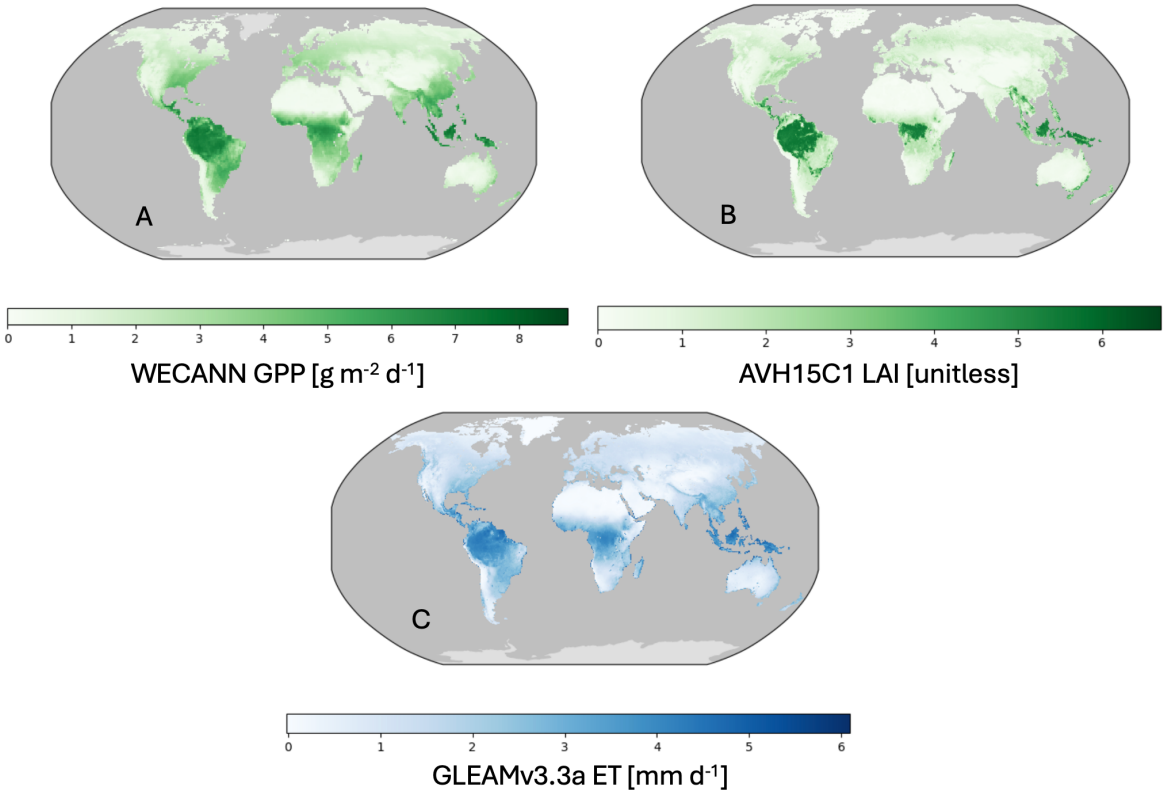

200

Figure 2: Long-term mean ecohydrological variables from observational datasets. (A) WECANN GPP [g m⁻² d⁻¹] (2007–2016), providing global estimates of gross primary productivity derived from machine learning techniques. (B) AVH15C1 LAI [unitless] (1981–2019), representing global leaf area index values from the NOAA Climate Data Record. (C) GLEAMv3.3a ET [mm d⁻¹] (1980–2018), showing global evapotranspiration estimates derived from
205 **satellite observations and meteorological data. Each subplot displays the global distribution of these ecohydrological variables.**

While ILAMB supports multiple observational datasets for each variable, we utilize a single benchmark dataset per variable in this study to maintain consistency and simplicity in our analysis. It is worth noting that although these products are widely used as observational references, they are themselves derived from models or statistical algorithms informed by
210 observational inputs. As such, they should be interpreted as observationally informed estimates rather than direct measurements. Nonetheless, these datasets provide reliable and widely accepted benchmarks for evaluating modeled GPP, LAI, and ET (represented by the gpp, lai, and evspsbl variables), supporting a comprehensive evaluation of ecohydrologic processes and their relationships with SM.

https://doi.org/10.5194/egusphere-2025-3517
Preprint. Discussion started: 10 September 2025

2.4 ILAMB Framework

The ILAMB framework is an open-source software package used to assess the performance of ESMs by comparing model outputs to a suite of observational datasets. ILAMB's scoring system integrates several key performance metrics: bias, RMSE, seasonal cycle representation, and spatial distribution (Figure A1). These metrics are synthesized into an overall score using the method detailed in Collier et al. (2018), offering a quantitative view of model fidelity. Bias measures the average deviation from observational data, RMSE quantifies error magnitude, and the seasonal cycle and spatial metrics assess the temporal and geographic accuracy of model outputs. By combining these metrics, ILAMB generates diagnostic graphics and scores to help identify strengths and weaknesses in model simulations. The ILAMB framework has been widely adopted for model evaluation and intercomparison, aiding in the continuous development of more accurate land model components (Collier et al., 2018, 2023).

In this study, we extend the ILAMB analysis by incorporating Köppen climate classifications, which allows for a more detailed evaluation of model performance across diverse climate zones. These regions, which include tropical, desert and semi-arid, temperate, and continental climates, reflect varying environmental conditions that significantly influence SM and vegetation dynamics. By examining model skill within these distinct climate zones, we gain deeper insights into region-specific strengths and weaknesses, allowing for targeted improvements in land models across climate types.

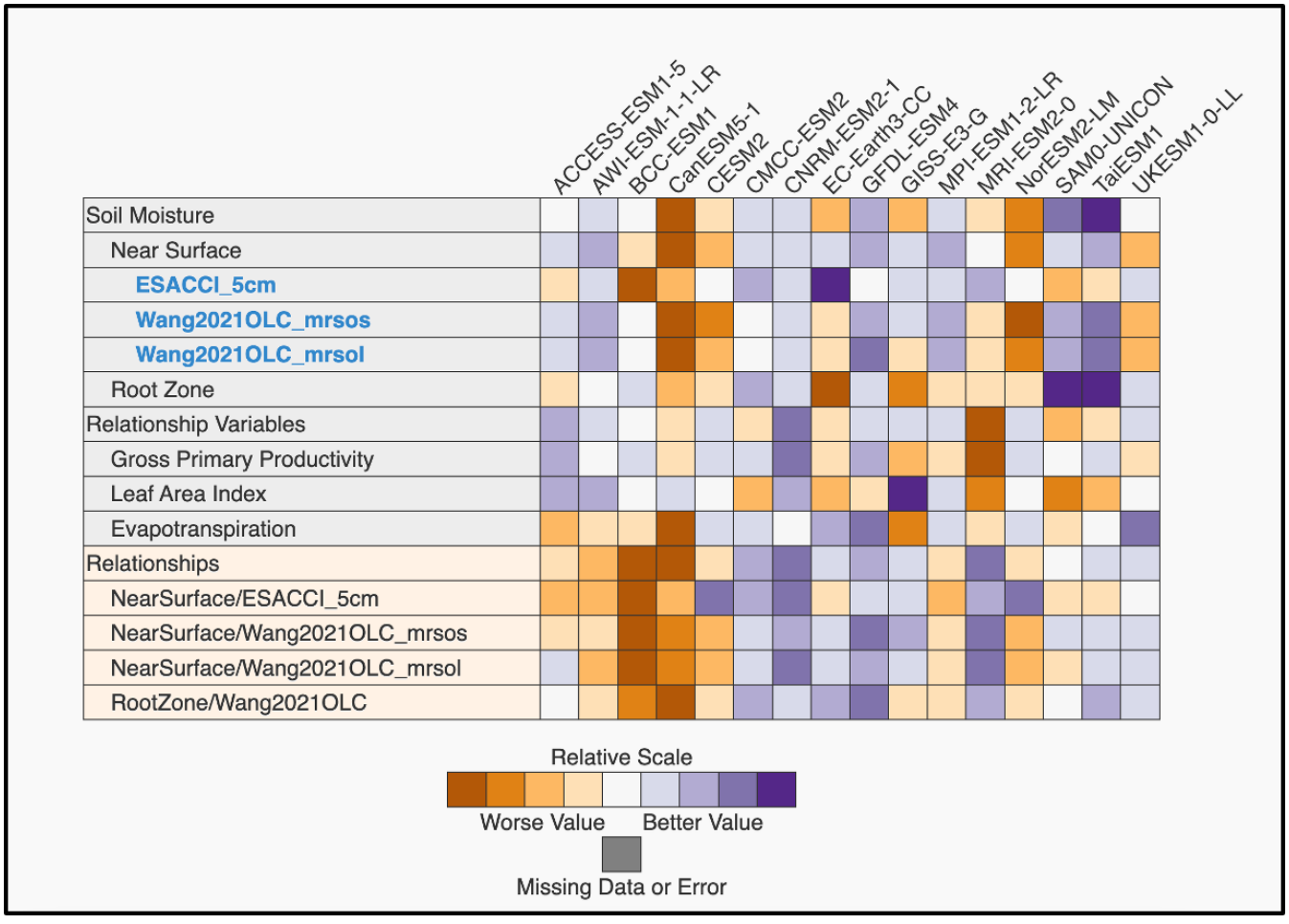

https://doi.org/10.5194/egusphere-2025-3517
Preprint. Discussion started: 10 September 2025

Figure 3: Benchmarking results from the ILAMB global run. Each model is compared against observational datasets: ESA-CCI Surface SM [$m^3\ m^{-3}$] (top 5 cm), Wang2021OLC Surface SM [$m^3\ m^{-3}$] (top 10 cm), Wang2021OLC Rootzone SM [$m^3\ m^{-3}$] (top 100 cm), WECANN GPP [$g\ m^{-2}\ d^{-1}$], AVH15C1 LAI [unitless], and GLEAMv3.3a ET [$mm\ d^{-1}$]. Additionally, the relationships between soil moisture and ecohydrological variables (GPP, LAI, and ET) are also benchmarked. Purple represents better relative skill, while orange indicates relatively worse performance.

3 Results from ILAMB

3.1 Overall benchmark scores in ILAMB

In this section, we present the evaluation of CMIP6 model performance using the ILAMB framework, focusing on key land surface variables. Specifically, we benchmark model outputs against observational datasets for surface and rootzone SM, as well as ecohydrological variables. Surface SM is evaluated using the ESA-CCI product (top 5 cm, Figure 1A) and the Wang2021OLC dataset (top 10 cm, Figure 1B), while rootzone SM (up to 100 cm) is assessed using the Wang2021OLC product (Figure 1C). For ecohydrological benchmarking, we use GPP from WECANN (Figure 2A), LAI from AVH15C1 (Figure 2B), and ET from GLEAMv3.3a (Figure 2C).

Overall model performance across these variables is summarized in the ILAMB portrait plot (Figure 3), where models are color-coded from orange (lower performance) to purple (higher performance). These benchmarks are derived from quantitative ILAMB evaluation metrics, including the Bias Score, RMSE Score, Seasonal Cycle Score, and Spatial Distribution Score. These scores contribute to the final benchmark, represented as the Overall Score, and are the results that are presented in Figure 3. Figure A1 shows these metrics based on global SM simulations using the mrsol variable integrated to 10 cm, compared against the Wang2021OLC dataset at the same depth. Figure A2 presents the quantitative overall ILAMB scores used to generate the colored portrait plot in Figure 3. Figure A3 shows global maps of model bias ($m^3\ m^{-3}$), calculated as the difference between simulated and observed surface SM (mrsol to 10 cm vs. Wang2021OLC top 10 cm), providing spatial insight into model performance. While the results in Figure 3 and Figures A1-A3 show the overall quantitative benchmarking scores generated with ILAMB, the following subsections provide a more detailed analysis of model performance across SM, ecohydrological variables, and their interrelationships.

3.2 Surface and Rootzone Soil Moisture

The evaluation of surface SM using both ESA-CCI (top 5 cm) and Wang2021OLC (top 10 cm) datasets shows broad agreement in overall model rankings (Figure 3), indicating consistent model performance across shallow soil depths. This consistency extends to rootzone SM (0–100 cm) when assessed using the Wang2021OLC dataset, suggesting that several models are generally stable in their representation of SM across soil layers. However, notable discrepancies emerge depending on the benchmark dataset used. Some models perform well relative to ESA-CCI but show significantly lower skill against Wang2021OLC, particularly for rootzone SM. Conversely, other models show improved performance when benchmarked against Wang2021OLC compared to ESA-CCI. This variation underscores the sensitivity of model evaluation to the choice of reference dataset and highlights the need for multi-dataset benchmarking.

https://doi.org/10.5194/egusphere-2025-3517
Preprint. Discussion started: 10 September 2025

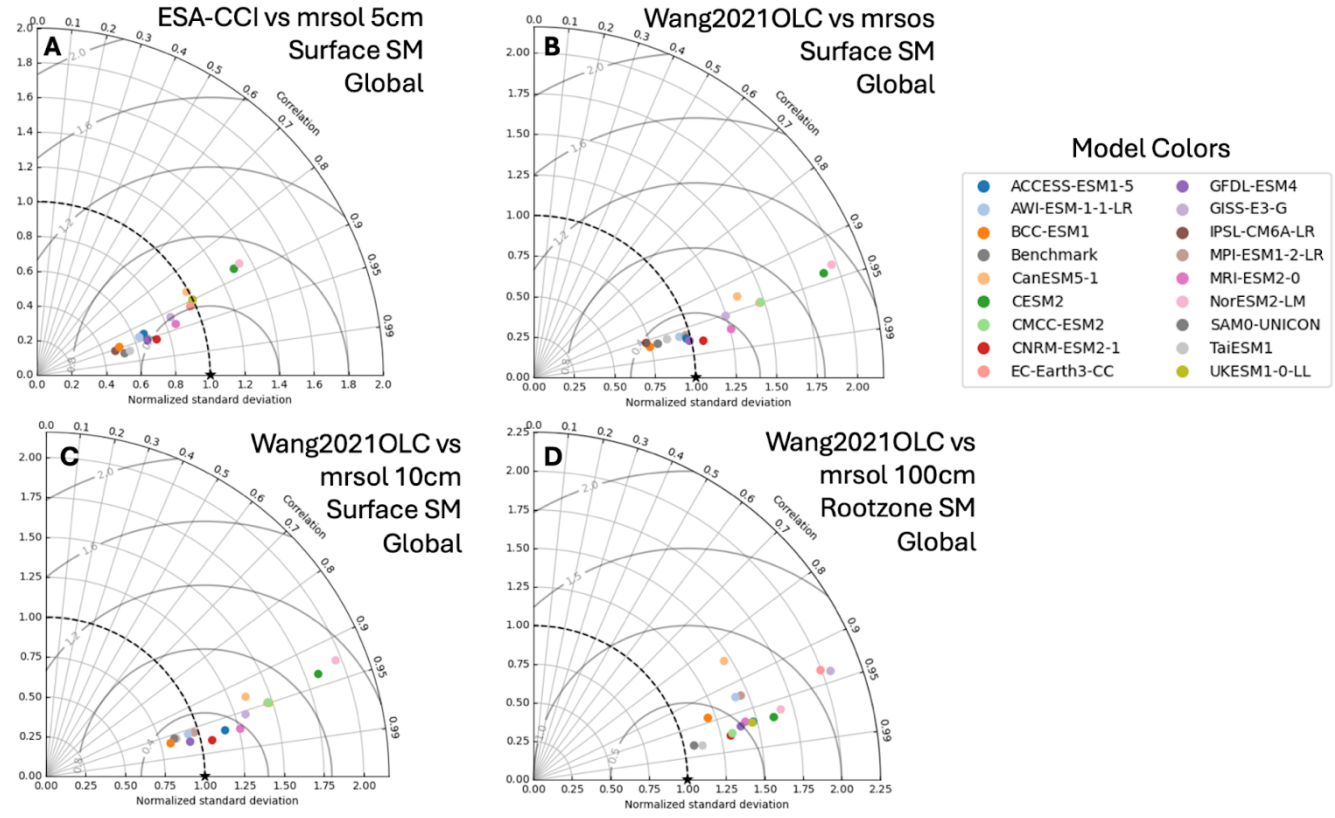

Figure 4: Taylor diagrams evaluating the performance of CMIP6 model SM simulations compared to different observational datasets: A) Surface SM from ESA-CCI (top 5 cm), B) Wang2021OLC Surface SM using mrsos from the models (top 10 cm), C) Wang2021OLC Surface SM using mrsol from the models (top 10 cm), and D) Wang2021OLC Rootzone SM (top 100 cm).

Figure 4 presents Taylor diagrams comparing model performance against the four SM benchmark datasets used in this study. These diagrams show that models generally capture the correlation and spatial patterns of surface SM well, though with varying degrees of bias and spread. The results show that models exhibit greater skill in capturing correlations than standard deviations, suggesting they better represent relative wetness and dryness patterns than absolute soil moisture levels. Furthermore, the evaluation of the mrsos and mrsol to 10 cm SM exhibits similar but non-identical model performance, verifying the difference between the two variables (Figure 4BC). In contrast to surface SM, rootzone SM exhibits systematic overestimation of variability across all models. This tendency suggests that ESMs simulate larger fluctuations in deeper SM than are observed, pointing to a key area for improvement in land surface hydrology representations. However, the scarcity of observations for deeper SM likely contributes to the smaller observed variability at this depth, suggesting that part of the model–data discrepancy may stem from limited observational coverage.

3.3 Ecohydrological Variables

The evaluation of ecohydrological variables (GPP, LAI, and ET) reveals limited consistency in model performance across these variables (Figure 3). That is, models that perform well in simulating one variable often perform poorly in others. This results in a wide spread of rankings, with few models consistently performing well across all three benchmarks. For instance,

https://doi.org/10.5194/egusphere-2025-3517
Preprint. Discussion started: 10 September 2025

while some models demonstrate relatively strong performance across GPP, LAI, and ET, others excel in only one variable or underperform across all variables, highlighting the challenge of achieving balanced ecohydrological realism in ESMs.

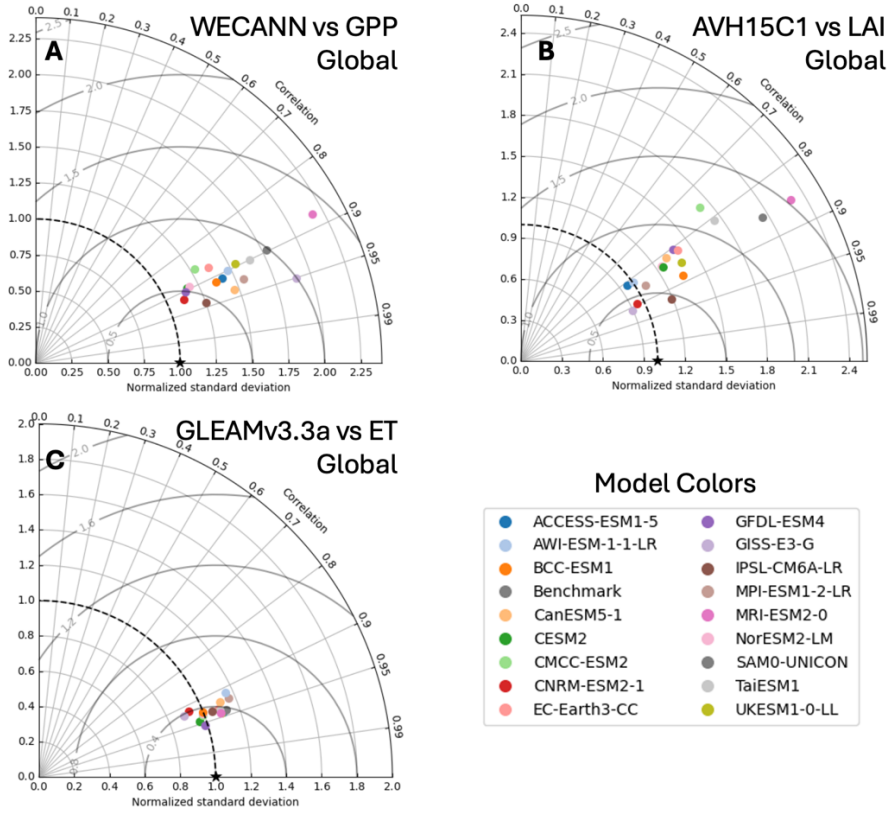

Figure 5: Taylor diagrams evaluating the performance of CMIP6 models in simulating ecohydrologic variables: A) Gross Primary Productivity (GPP) from WECANN, B) Leaf Area Index (LAI) from AVH15C1, and C) Evapotranspiration (ET) from GLEAMv3.3a.

Taylor diagrams in Figure 5 provide a more detailed comparison of model performance against the ecohydrological observational datasets. Across most models, a systematic high bias in variability is evident for both GPP and LAI, suggesting that models tend to overestimate fluctuations in vegetation productivity and canopy structure. In contrast, model simulations of ET show stronger agreement with observations, both in terms of variability and spatial correlation. This comparatively better performance in ET may reflect stronger observational constraints and more developed parameterizations in hydrologic and surface energy fluxes. However, it may also indicate compensating errors within model processes or parameters that mask deficiencies in SM representation. By comparison, vegetation-related processes such as carbon uptake and phenology likely carry greater structural uncertainty (Massoud et al., 2019; Li et al., 2025b), contributing to more pronounced biases in GPP and LAI.

3.4 Relationship of Soil Moisture to Ecohydrological Variables

Figures 6 and 7 illustrate the relationships between SM and key ecohydrological variables (GPP, LAI, and ET) for the ACCESS-ESM1-5 model, comparing model outputs to two different observational SM products. Figure 6 uses the ESA-CCI surface SM product (0–5 cm) alongside model SM integrated to the same depth (mrsol to 5 cm). The dot-and-whisker plots

https://doi.org/10.5194/egusphere-2025-3517
Preprint. Discussion started: 10 September 2025

reveal notable discrepancies between model (blue) and observations (black), indicating areas where the model may misrepresent vegetation sensitivity to near-surface SM.

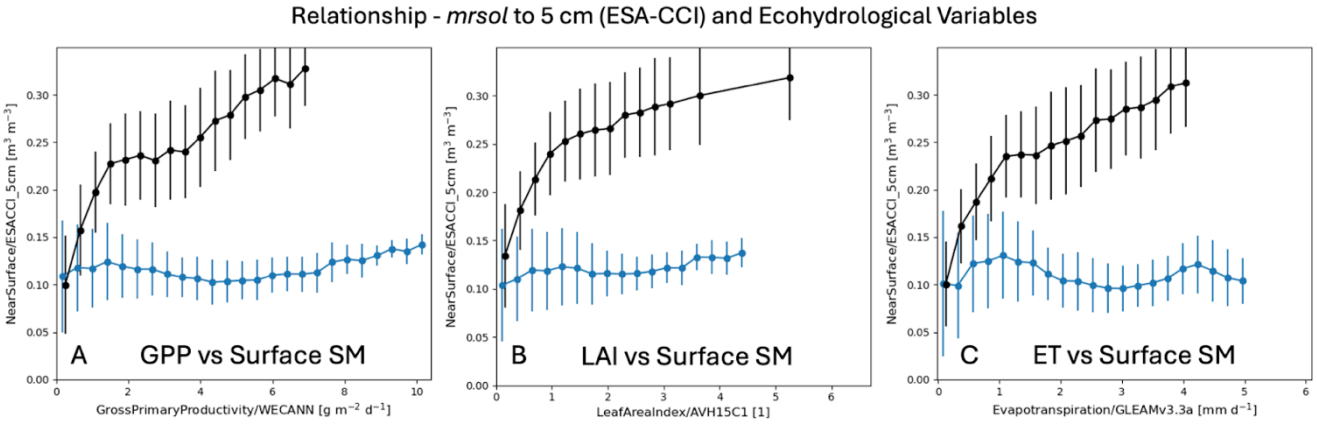

Figure 6: Relationship of SM (y-axis) versus ecohydrological variables (x-axis) shown through dot-and-whisker plots for the ACCESS-ESM1-5 model (blue) and observations (black). The ESA-CCI SM product (typically to 5 cm) is used here for SM, compared to the ACCESS-ESM1-5 model's SM integrated to the same depth (mrsol to 5 cm). The relationship of these SM estimates are shown for (a) WECANN GPP, (b) AVH15C1 LAI, and (c) GLEAMv3.3a ET at the global scale. Whiskers indicate interquartile ranges across land grid cells. These plots reveal a significant discrepancy between the model and observations when using ESA-CCI as the SM benchmark.

Figure 7 presents an analogous analysis using the Wang2021OLC SM product (top 10 cm) and model SM integrated to the same depth (mrsol to 10 cm). Here, models show improved agreement with observations across all ecohydrological variables, suggesting that part of the mismatch seen with ESA-CCI may stem from differences in observational datasets or soil depth representation. However, it is important to note that the ILAMB spatial climatology used in Figures 6 and 7 may be affected by ESA-CCI's inconsistent spatiotemporal coverage (c.f., Preimesberger et al., 2025), potentially biasing its evaluation. Conversely, Wang2021OLC relies heavily on reanalysis data, which incorporates model structures and may thus reduce apparent model biases by design. Despite this improvement, persistent biases highlight ongoing challenges in accurately simulating SM–vegetation coupling within ESMs.

Extending this comparison across all models, Figure 8 shows SM–GPP relationships for the full CMIP6 ensemble using mrsol to 10 cm and the Wang2021OLC and WECANN datasets. Consistent with ACCESS-ESM1-5 results, models generally exhibit better agreement when benchmarked against Wang2021OLC compared to ESA-CCI (as in Figure 6), further validating the utility of Wang2021OLC for evaluating SM–vegetation coupling. These findings highlight both the strengths and limitations of current Earth System Models in representing key ecohydrological interactions, while demonstrating the value of ILAMB for detailed inter-model diagnostics.

https://doi.org/10.5194/egusphere-2025-3517
Preprint. Discussion started: 10 September 2025

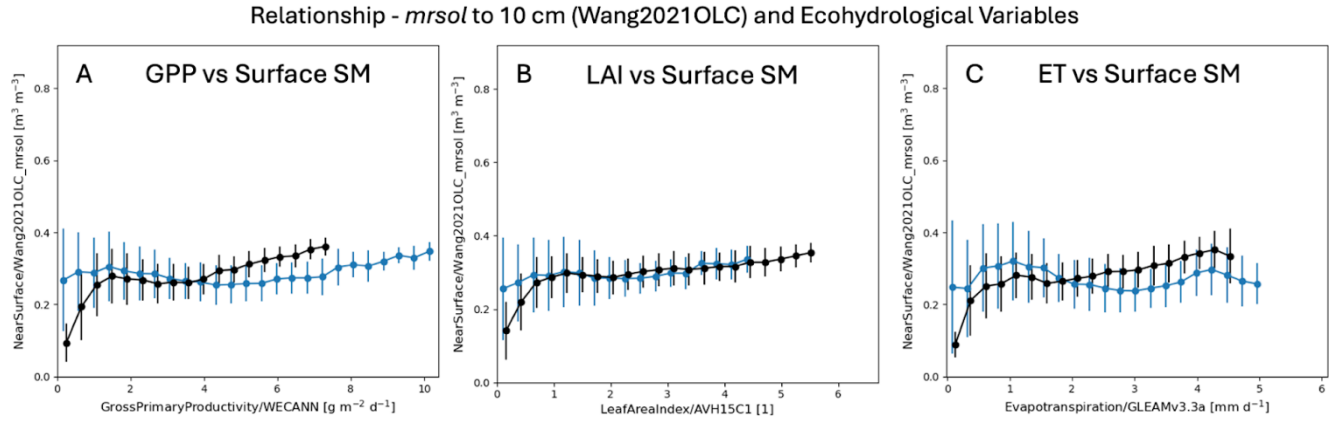

Figure 7: Similar to Figure 6, but using the Wang2021OLC SM product (integrated to 10 cm) and the corresponding ACCESS-ESM1-5 model SM at the same depth (mrsol to 10 cm). Dot-and-whisker plots show the relationship of soil moisture (y-axis) versus (a) WECANN GPP, (b) AVH15C1 LAI, and (c) GLEAMv3.3a ET for both model (blue) and observations (black) at the global scale. Whiskers represent interquartile ranges. Compared to Figure 6, these plots demonstrate a marked reduction in discrepancies between modeled and observed relationships.

3.5 Other ILAMB capabilities: Köppen Classification

While the preceding analyses focus on global-scale benchmarking (which is the default in ILAMB) one of ILAMB's key strengths is its ability to evaluate model performance across specific biogeographic zones. Using Köppen classifications, ILAMB enables targeted regional analysis across zones such as Tropical, Desert and Semi-arid, Temperate, and Continental climates. Figure A4 illustrates these regions and shows regional mean values of surface SM from the ESA-CCI product to provide geographic context.

https://doi.org/10.5194/egusphere-2025-3517
Preprint. Discussion started: 10 September 2025

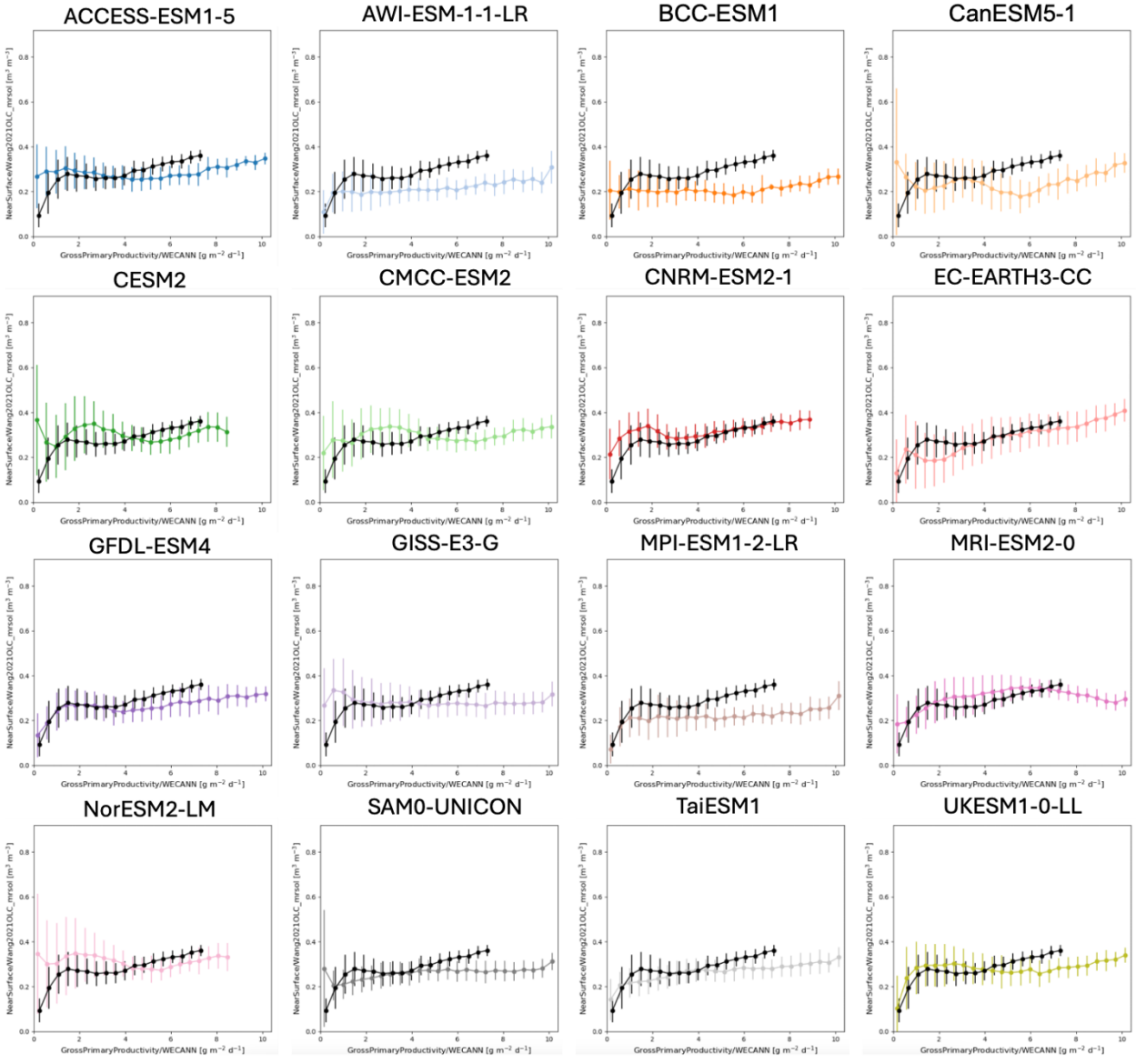

Figure 8: Similar to the bias plots shown in Figure 7A, but for all models. These plots highlight the observed relationships (black curves) between the surface SM (from the Wang2021OLC top 10 cm SM product) and GPP (from WECANN), as well as the relationship shown in each model (colored curves) using the simulated mrsol to 10 cm and gpp variables.

To demonstrate the utility of regional benchmarking, Figure A5 presents ILAMB portrait-style evaluations (using the same methodology as Figure 3) and Figure A6 shows the evaluated relationships for the Tropical region (using the same methodology as Figures 6-7). The ILAMB portrait-style evaluations for the remaining Köppen regions are shown in Figure A7 (Desert and semi-arid), A8 (Temperate), and A9 (Continental), again using the same methodology as Figure 3.

https://doi.org/10.5194/egusphere-2025-3517
Preprint. Discussion started: 10 September 2025

These localized portraits highlight how model performance can vary significantly by region. For example, some models like CESM2 and NorESM2-LM exhibit a high bias in high northern latitudes when evaluated globally (as depicted in Figure A2), yet perform relatively well in the Tropical region (Figure A5). Conversely, their performance declines in the Continental zone (Figure A8). EC-Earth3-CC scores highly in the Tropical region when evaluated against ESA-CCI but ranks among the lowest when evaluated against the Wang2021OLC dataset for the same region, highlighting uncertainty in the benchmarking datasets in the region. In contrast, it shows more consistent agreement across both observational products in Continental areas.

ILAMB's regional diagnostics also extend to ecohydrological relationships. Figure A6 mirrors the SM–ecohydrology analysis shown in Figure 7 but focuses specifically on the Tropical region and surface SM. In this example, the ACCESS-ESM1-5 model shows reasonably good agreement with observed relationships in the Tropical region when evaluated against the Wang2021OLC dataset. This supports earlier findings that surface SM comparisons with Wang2021OLC tend to yield consistent model–observation alignment. These regional results further emphasize the value of localized analyses for identifying where models are performing well and where region-specific improvements are needed.

4 Discussion

4.1 Potential Drivers for Divergences in Model Simulations

The substantial spread in SM estimates among CMIP6 models reflects differences in how land surface models (LSMs) represent key processes and input data. Although precipitation is a major driver of SM, it does not explain much of the mean inter-model variability in this study. Most CMIP6 models simulate similar global mean precipitation rates of approximately 2.5 mm/day (Tapiador et al., 2018), suggesting that differences in total precipitation alone are insufficient to account for the spread in simulated SM (see Figure A1, column 'Model Period Mean'). However, the timing and intensity of precipitation events, rather than total amounts, may contribute significantly to model divergence, especially in regions with highly seasonal precipitation regimes where the timing of precipitation governs the length of dry-down periods. This effect is particularly pronounced in seasonally snowmelt-dominated systems (Harpold et al., 2015), where variations in precipitation and snowmelt seasonality strongly influence the partitioning between infiltration, runoff, and ET. Differences in how models represent storm frequency, sub-daily rainfall variability, and snowmelt dynamics can further impact SM through their interactions with soil hydrology and vegetation water uptake. Future work should investigate the role of precipitation and snowmelt timing, along with event-scale dynamics, in driving model spread.

Similarly, the treatment of soil ice is unlikely to contribute significantly to SM variability, as the CMIP6 definition of SM includes both liquid water and ice, which should be handled consistently across models and only present in cold areas with minimum snow cover. This implies that other factors, such as soil properties, hydrologic parameterizations, and land-atmosphere feedbacks, are likely more important contributors.

One important driver is the treatment of soil properties, particularly in high-latitude regions. Models that include representations of organic soils, such as CESM2 and NorESM2-LM, tend to simulate higher SM levels, likely due to the greater water-holding capacity of organic matter. Both models use the CLM5 land surface scheme, which explicitly accounts for organic soil processes in northern latitudes (Lu et al., 2020). This feature may explain the higher SM values observed in these models' bias maps (e.g., Figure A3). However, the inclusion of organic soils in CESM2 and NorESM2-LM models may have led to better SM representation in the tropics (Figure A5), where organic soil is prevalent in the tropical forests. It remains unclear whether all CMIP6 models have updated their treatment of organic soils, which could contribute to persistent inter-model differences.

Soil porosity is another critical input affecting SM simulations. Previous work (Dai et al., 2019) has shown that many CMIP5 models used outdated soil maps (e.g., FAO-UNESCO, 1981), and some CMIP6 models may still rely on these

https://doi.org/10.5194/egusphere-2025-3517
Preprint. Discussion started: 10 September 2025

legacy datasets. More modern and accurate global soil datasets, such as the Harmonized World Soil Database v2.0 (Nachtergaele et al., 2023), the Global Soil Dataset for Earth System Modeling (Shangguan et al., 2014), and SoilGrids (Hengl et al., 2014), offer improved estimates of soil properties, including porosity. Comparing SM outputs against these updated datasets could help reveal systematic biases tied to inaccurate soil input data.

Model-specific representation of hydrologic processes can also influence SM estimates. For example, the EC-Earth3-CC model consistently simulates high SM values, potentially due to its inclusion of groundwater–soil interactions not present in other models. With a few exceptions (Oleson et al., 2013; Lawrence et al., 2019), ESMs generally use 'bucket type' soil moisture representations that drain water between different soil layers based on predefined thresholds (e.g., field capacity) and rates (e.g., hydraulic conductivity) rather than the pressure-driven movement represented by more physically-based models like the Richard's Equation. Although ESMs differ, several key processes and parameters are common and should be considered in model performance differences: number and spacing of soil layers, rooting profile and ET process representation, infiltration process representation, soil properties (i.e. porosity, wilting point and field capacity water content at each layer, and hydraulic conductivity), and soil depth and the bottom boundary condition (e.g., groundwater versus freely draining). Such process-level differences highlight the role of internal model design in shaping SM outputs that remain challenging to disentangle.

Finally, land-atmosphere feedbacks may also contribute to the inter-model spread. CMIP models have been shown to overestimate the strength of feedbacks between SM and atmospheric variables, including temperature, ET, and surface fluxes (Levine et al., 2016). These exaggerated feedbacks may amplify SM variability and introduce additional divergence across models. For instance, models that strongly couple soil moisture to surface heat fluxes may simulate more aggressive drying or wetting cycles, depending on local conditions (Schumacher et al., 2022). The degree of inter-model variability in feedback strength is probably quite high, but more studies will be needed to understand how this affects inter-model spread in SM (Vogel et al., 2016; Talib et al., 2023). Further research is needed to examine how different models simulate the sensitivity of ET and energy partitioning to meteorological conditions such as vapor pressure deficit, solar radiation, or wind speed, factors that could also shape SM variability via land-atmosphere interactions.

In summary, the observed variability in SM simulations across CMIP6 models likely stems from a combination of factors, including differences in soil properties, legacy input datasets, precipitation event timing, hydrologic parameterizations and process representations, and feedback mechanisms. Future research should aim to disentangle the relative contributions of these drivers to better constrain SM representation in ESMs.

4.2 Shared characteristics of models with similar performance

Models that exhibit similar performance across multiple variables often share underlying structural and process-based characteristics. For example, CESM2 and NorESM2-LM, while performing relatively poorly in simulating SM (e.g., Figure 3), show stronger agreement with observations for ecohydrological variables such as GPP, LAI, ET. A shared feature of these models is their use of the CLM5, which likely contributes to their consistent performance in simulating vegetation dynamics and surface fluxes. However, despite these strengths, both models apparently exhibit a persistent high-latitude bias in SM (Figure A3), likely related to CLM5's representation of soil properties and its inclusion of organic matter in northern soils (Lu et al., 2020). However, considering the bias of satellite observations under snow- and ice-covered conditions (Dorigo et al., 2015) and the relatively high influence of reanalysis and land surface models on the Wang2021OLC product (Wang et al. 2021), this bias in high-latitudes warrants further investigation with more observational datasets.

In addition to similarities in their overall performance scores, CESM2 and NorESM2-LM also exhibit relatively consistent relationships between SM and ecohydrological variables. These relationships, such as SM-GPP and SM-ET coupling, reflect each model's ability to capture key land-atmosphere feedbacks, including how soil water availability influences stomatal conductance, photosynthetic rates, and vegetation phenology. Notably, this suggests that even when absolute SM values are biased, some models may still effectively represent the underlying functional dynamics between water and vegetation. In

https://doi.org/10.5194/egusphere-2025-3517
Preprint. Discussion started: 10 September 2025

contrast, models with weaker SM performance tend to display greater mismatches in these coupling relationships, indicating broader limitations in their ability to simulate ecohydrological processes.

Taken together, these patterns highlight that model performance is influenced not only by how individual processes are parameterized, but also by how different components of the land system interact. Structural choices, such as vegetation and soil representations, hydrologic schemes, and coupling strategies, shape a model's capacity to simulate both state variables and their interrelationships. As such, evaluating models across multiple variables and focusing on cross-variable coherence can provide deeper diagnostic insight than isolated benchmark scores. These shared behaviors among models with similar architectures may point to areas where coordinated model development and targeted improvements, such as refining soil parameterizations or vegetation-hydrology interactions, could yield broad performance gains.

4.3 Consideration of uncertainty in the benchmark results

Evaluating model performance inherently involves uncertainty, both from observational datasets and model representations. To better characterize this uncertainty, we employed multiple observational products for surface and rootzone SM, including ESA-CCI and Wang2021OLC surface SM, as well as Wang2021OLC rootzone SM. By comparing models against more than one observational reference, we aimed to capture a broader envelope of observational variability, rather than relying on any single product that may contain its own structural or systematic biases. Similarly, we assessed different model representations of SM, including the mrsos and mrsol variables integrated to 5 cm, 10 cm, and 100 cm depths, to examine how model configuration affects evaluation outcomes.

Soil moisture presents unique challenges in benchmarking due to the diversity and limitations of observational data sources. Satellite-derived products, for example, offer broad spatial coverage but are limited to shallow depths and may have coarser resolution for passive microwave technology, whereas active microwave technology can achieve higher resolution but is subject to greater uncertainty from surface roughness and vegetation structure variations (Zeng et al., 2023). In contrast, in-situ observations provide deeper and more accurate point measurements but are geographically sparse and face the scaling-up problem when compared against ESMs. While our study did not include in-situ datasets, their inclusion could strengthen future benchmarks by adding another layer of observational comparison, particularly for deeper soil layers. The variation in spatial resolution, vertical depth coverage, and methodological differences between observational datasets contributes to uncertainty in benchmarking, and any conclusions drawn from SM comparisons should be interpreted within this context.

To address these complexities, we adopted a multi-product comparison approach. However, additional strategies exist and may further enhance benchmarking efforts. In atmospheric science, for example, it is common to evaluate models not only against individual datasets but also against an ensemble of observations (Yamaguchi et al., 2015), which helps define a consensus observational baseline. While this strategy is less frequently used in the SM modeling community, it may offer a valuable pathway forward, particularly when observational datasets diverge or when no single product can be considered definitively superior.

Beyond observational uncertainty, ensemble modeling (using a collection of model runs or parameter sets) can also help characterize structural and parametric uncertainty within the models themselves. While not implemented in this study, future benchmarking efforts could benefit from integrating probabilistic or ensemble-based approaches to better understand model sensitivity (c.f., Massoud et al., 2019) and confidence in simulated soil moisture.

5 Conclusion

This study evaluated the performance of 16 CMIP6 models in simulating key land surface and ecohydrological variables, including surface and rootzone SM, GPP, LAI, and ET, using the ILAMB framework. The main findings are summarized as follows:

https://doi.org/10.5194/egusphere-2025-3517
Preprint. Discussion started: 10 September 2025

(i) Our analysis showed substantial variability in model performance in simulating SM, particularly when compared against more than one observational dataset. For instance, models such as EC-Earth3-CC performed well against ESA-CCI surface SM observations but underperformed when benchmarked against the Wang2021OLC dataset. This stresses the importance of using multiple observational products to better capture uncertainty and avoid drawing conclusions based on a single reference dataset.

(ii) Models often showed differing levels of skill across variables. For example, CESM2 and NorESM2-LM exhibited strong performance in ecohydrological variables like GPP, LAI, and ET, but showed consistent SM biases in high-latitude regions. These shared behaviors likely reflect common model structures, as both rely on the CLM5 land surface model. This highlights how model architecture and parameterizations influence simulation outcomes.

(iii) Beyond individual variables, we examined the relationships between soil moisture and ecohydrological processes. This analysis revealed that models tended to capture these relationships more effectively when compared to the Wang2021OLC dataset than to ESA-CCI, indicating that deeper or better-integrated soil moisture estimates may provide a more consistent benchmark for evaluating vegetation-water coupling.

(iv) The regional analysis using Köppen climate zones demonstrated ILAMB's capacity to localize model evaluations. Results showed that model skill can vary significantly by region. For instance, CESM2 and NorESM2-LM performed relatively well in tropical zones but struggled in continental regions. This highlights the need to move beyond global averages to uncover spatially varying model behavior. Regional benchmarking enables more precise identification of where and why individual ESMs succeed or fall short.

Overall, our findings showcase the strengths and limitations of current CMIP6 models in simulating land surface and ecohydrological processes. While some models excel in specific areas, no single model performs best across all metrics or regions. The ILAMB framework provides a powerful, systematic approach for benchmarking not only model outputs but also functional relationships among variables. This study also reinforces the value of considering multiple observational products and model configurations to account for uncertainty in benchmarking efforts.

Future work should continue to expand benchmarking approaches by incorporating in-situ observations, applying ensemble-based and probabilistic methods for both models and observational datasets, and further refining regional analyses. Ensemble approaches, in particular, can help quantify structural uncertainty and improve robustness in performance assessments by leveraging the diversity across models and observational products. Such efforts will be critical for improving our understanding of SM and land-atmosphere interactions and enhancing the development of next-generation ESMs.

https://doi.org/10.5194/egusphere-2025-3517
Preprint. Discussion started: 10 September 2025

Appendix

		Download Data	Period Mean (original grids) [m3 m-3]	Model Period Mean (intersection) [m3 m-3]	Benchmark Period Mean (intersection) [m3 m-3]	Model Period Mean (complement) [m3 m-3]	Benchmark Period Mean (complement) [m3 m-3]	Bias [m3 m-3]	RMSE [m3 m-3]	Phase Shift [months]	Bias Score [1]	RMSE Score [1]	Seasonal Cycle Score [1]	Spatial Distribution Score [1]	Overall Score [1]
Benchmark	[-]	0.240													
ACCESS-ESM1-5	[-]	0.251	0.246	0.240	0.307	0.227		0.00644	0.0557	1.72	0.379	0.506	0.752	0.962	0.621
AWI-ESM-1-1-LR	[-]	0.180	0.182	0.239	0.149	0.244		-0.0577	0.0699	1.28	0.278	0.567	0.824	0.974	0.642
BCC-ESM1	[-]	0.187	0.182	0.240	0.241	0.158		-0.0576	0.0723	1.36	0.265	0.525	0.811	0.939	0.613
CanESM5-1	[-]	0.217	0.203	0.240	0.370			-0.0364	0.0828	1.49	0.267	0.352	0.793	0.882	0.529
CESM2	[-]	0.282	0.278	0.240	0.333	0.188		0.0390	0.0726	1.21	0.377	0.498	0.831	0.637	0.578
CMCC-ESM2	[-]	0.251	0.249	0.240	0.285	0.199		0.00983	0.0625	1.22	0.378	0.493	0.830	0.841	0.607
CNRM-ESM2-1	[-]	0.271	0.267	0.240	0.316	0.180		0.0287	0.0573	1.21	0.365	0.482	0.842	0.984	0.631
EC-Earth3-CC	[-]	0.194	0.221	0.240	0.0717			-0.0201	0.0689	1.05	0.322	0.475	0.862	0.844	0.596
GFDL-ESM4	[-]	0.219	0.221	0.240	0.198			-0.0177	0.0516	1.37	0.376	0.562	0.807	0.981	0.658
GISS-E3-G	[-]	0.260	0.257	0.240	0.305	0.166		0.0198	0.0643	1.27	0.356	0.466	0.823	0.907	0.604
MPI-ESM1-2-LR	[-]	0.181	0.183	0.239	0.156	0.245		-0.0562	0.0679	1.35	0.277	0.576	0.811	0.978	0.644
MRI-ESM2-0	[-]	0.243	0.240	0.240	0.279	0.220		0.000579	0.0567	1.89	0.356	0.496	0.711	0.936	0.599
NorESM2-LM	[-]	0.289	0.287	0.240	0.301			0.0483	0.0829	1.26	0.345	0.476	0.825	0.631	0.550
SAM0-UNICON	[-]	0.229	0.215	0.240	0.405	0.181		-0.0236	0.0541	1.23	0.375	0.554	0.825	0.949	0.651
TaiESM1	[-]	0.218	0.218	0.240	0.212			-0.0216	0.0534	1.20	0.383	0.562	0.833	0.957	0.659
UKESM1-0-LL	[-]	0.207	0.207	0.240	0.200	0.212		-0.0314	0.0745	1.46	0.275	0.466	0.795	0.841	0.569

Figure A1: Evaluation of global simulations of SM using the *mrsol* variable to 10 cm, compared to the Wang et al. (2021) dataset at the same depth. The various metrics shown are the different benchmark scores used in the ILAMB evaluation, including Bias Score, RMSE Score, Seasonal Cycle Score, and Spatial Distribution Score. These scores contribute to the final benchmark, represented here as the Overall Score, and are the results that are presented in Figure 3 (and Figures S5 and S7-9).

https://doi.org/10.5194/egusphere-2025-3517
Preprint. Discussion started: 10 September 2025

	ACCESS-ESM1-5	AWI-ESM-1-1-LR	BCC-ESM1	CanESM5-1	CESM2	CMCC-ESM2	CNRM-ESM2-1	EC-Earth3-CC	GFDL-ESM4	GISS-E3-G	MPI-ESM1-2-LR	MRI-ESM2-0	NorESM2-LM	SAM0-UNICON	TaiESM1	UKESM1-0-LL
⊟ Soil Moisture	-0.25	0.54	-0.33	-2.31	-0.52	0.79	0.40	-0.78	0.84	-0.76	0.52	-0.22	-1.10	1.54	1.83	-0.20
⊞ Near Surface	-0.18	0.93	-1.35	-2.52	-0.54	0.48	0.58	0.82	1.11	0.13	1.04	0.12	-1.15	0.41	0.95	-0.84
⊞ Root Zone	-0.22	-0.03	0.74	-1.16	-0.28	0.74	0.07	-1.93	0.24	-1.25	-0.17	-0.44	-0.60	1.93	1.88	0.47
⊟ Relationship Variables	0.94	0.39	0.07	-0.62	0.57	-0.41	1.47	-0.37	0.65	0.68	0.21	-3.04	0.46	-1.02	-0.39	0.43
⊞ Gross Primary Productivity	1.01	-0.02	0.54	-0.32	0.55	0.55	1.27	-0.28	0.92	-0.87	-0.58	-3.16	0.50	-0.08	0.22	-0.26
⊞ Leaf Area Index	0.94	0.79	-0.11	0.14	0.05	-1.24	1.08	-0.78	-0.41	2.34	0.71	-1.66	0.09	-1.25	-0.81	0.10
⊞ Evapotranspiration	-0.99	-0.47	-0.61	-1.99	0.80	0.36	0.05	1.16	1.44	-1.42	0.23	-0.43	0.42	-0.49	0.08	1.89
⊟ Relationships	-0.25	-0.83	-2.02	-2.07	-0.26	0.85	1.16	0.50	1.20	0.15	-0.66	1.32	-0.23	-0.02	0.82	0.35
⊞ Near Surface/ESACCI_5cm	-0.81	-1.20	-1.85	-0.95	1.58	0.79	1.39	-0.36	0.20	0.37	-1.05	0.94	1.45	-0.30	-0.27	0.04
⊞ Near Surface/Wang2021OLC_mrsos	-0.47	-0.68	-2.17	-1.28	-1.07	0.63	1.21	0.36	1.36	0.79	-0.47	1.27	-0.89	0.57	0.57	0.26
⊞ Near Surface/Wang2021OLC_mrsol	0.65	-0.93	-1.90	-1.61	-0.78	0.71	1.42	0.38	0.92	0.62	-0.69	1.49	-0.86	-0.31	0.64	0.26
⊞ Root Zone/Wang2021OLC	-0.11	-0.53	-1.53	-2.54	-0.37	0.83	0.69	0.81	1.34	-0.38	-0.46	1.09	-0.29	-0.01	1.22	0.22

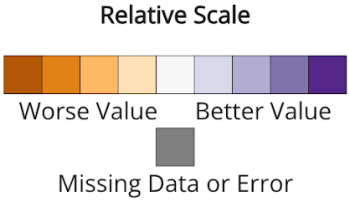

Figure A2: Overall scores that provide the ILAMB results in Figure 3 are depicted numerically here.

https://doi.org/10.5194/egusphere-2025-3517
Preprint. Discussion started: 10 September 2025

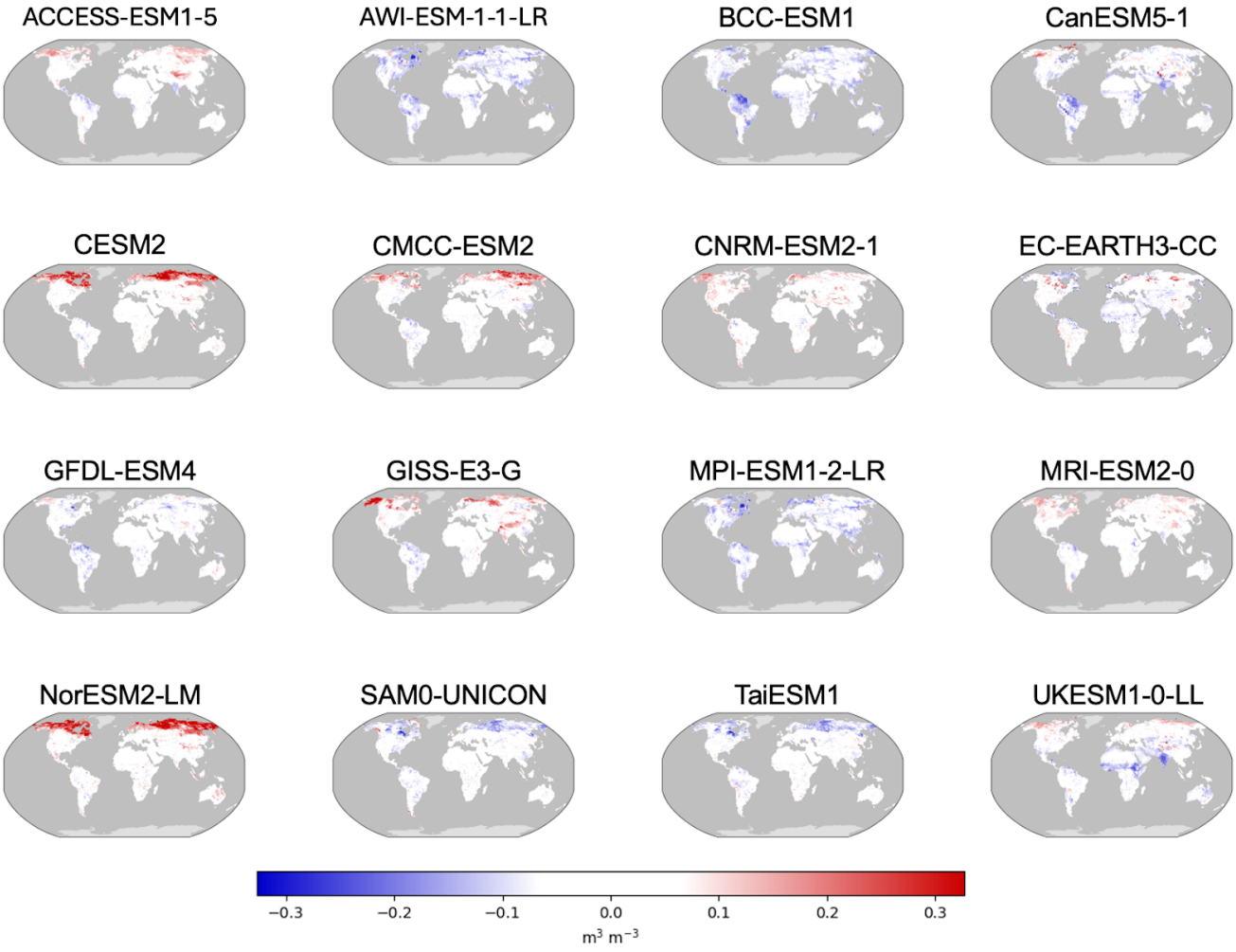

535 **Figure A3: Bias plots (in m³ m⁻³) comparing Wang2021OLC top 10 cm SM product to the *mrsol* variable up to 10 cm for all models. The bias is calculated as the difference between model simulations and observations in each grid cell, providing insight into simulated SM performance in various regions around the globe.**

https://doi.org/10.5194/egusphere-2025-3517
Preprint. Discussion started: 10 September 2025

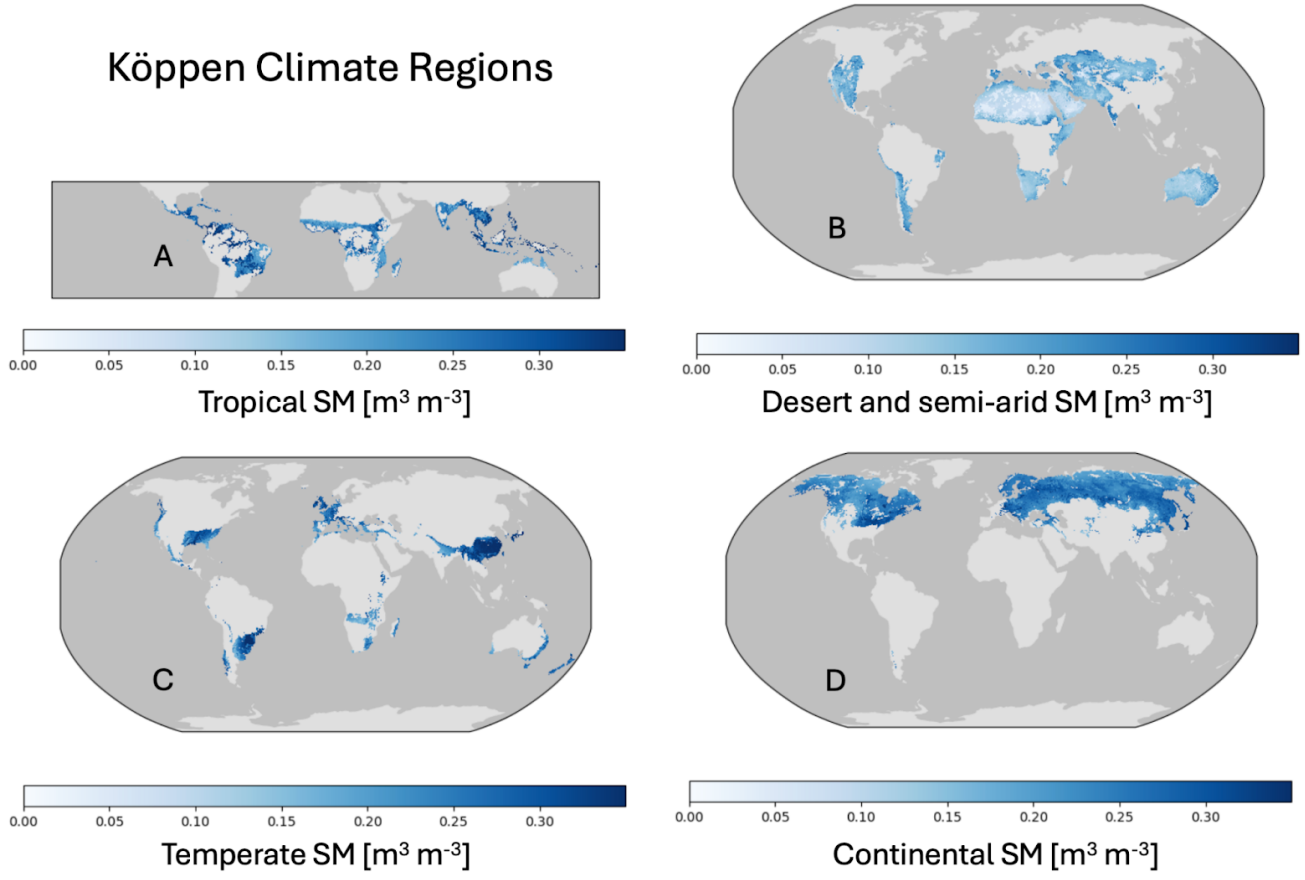

Figure A4: Köppen climate regions evaluated in this study through ILAMB. The default region is "global," while other regions include A) Tropical, B) Desert and Semi-arid, C) Temperate, and D) Continental. Regional mean values of surface SM derived from the ESA-CCI product are shown. The ESA-CCI dataset includes some data gaps, particularly in densely forested regions (e.g., the Amazon and Congo), ice-covered areas, and urban zones, due to limitations in microwave satellite observations. These gaps are more prevalent in earlier years and become less frequent over time. However, the primary purpose of this figure is to broadly illustrate the Köppen climate regions rather than serve as a detailed analysis of SM.

https://doi.org/10.5194/egusphere-2025-3517
Preprint. Discussion started: 10 September 2025

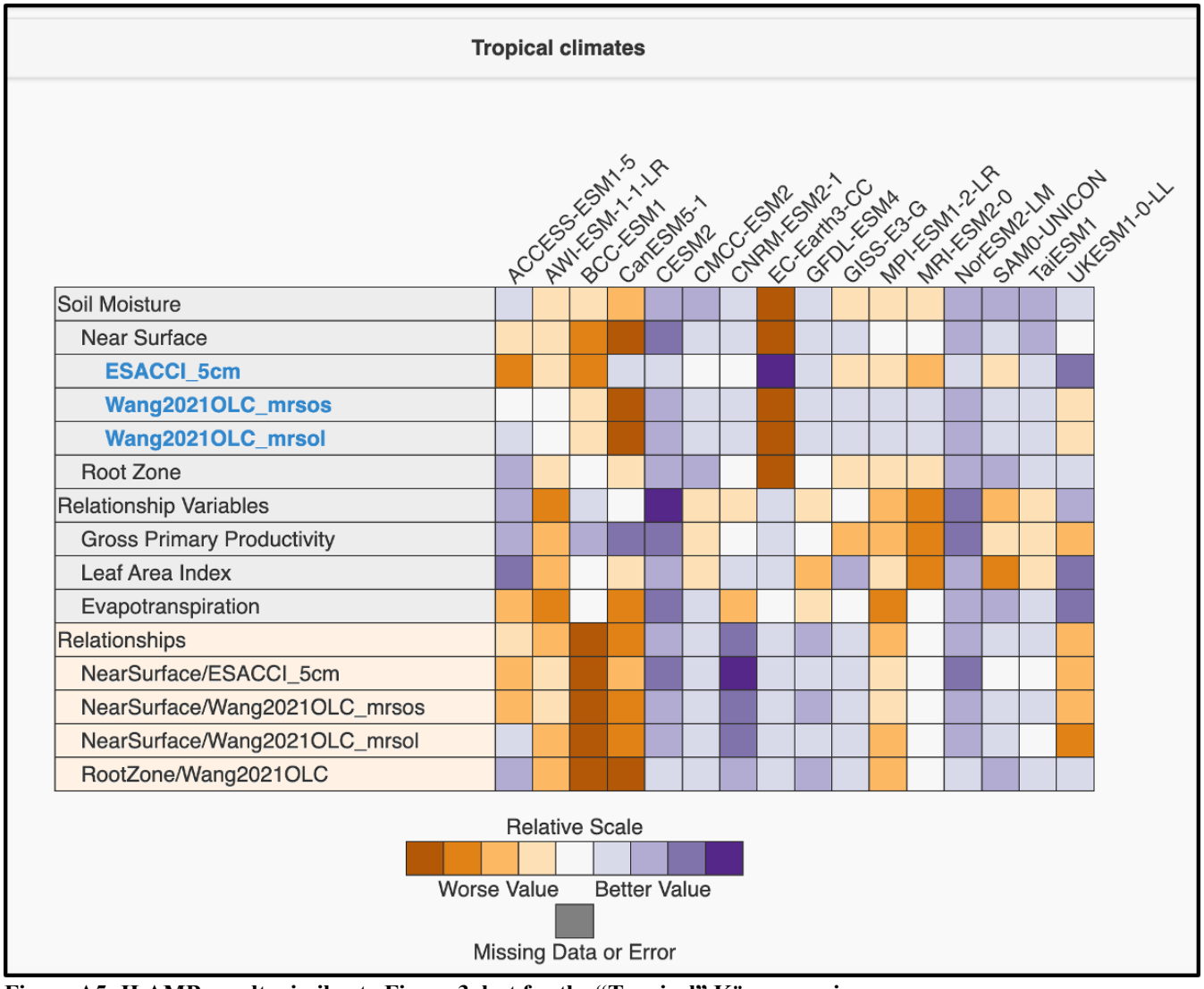

Figure A5: ILAMB results similar to Figure 3, but for the "Tropical" Köppen region.

https://doi.org/10.5194/egusphere-2025-3517
Preprint. Discussion started: 10 September 2025

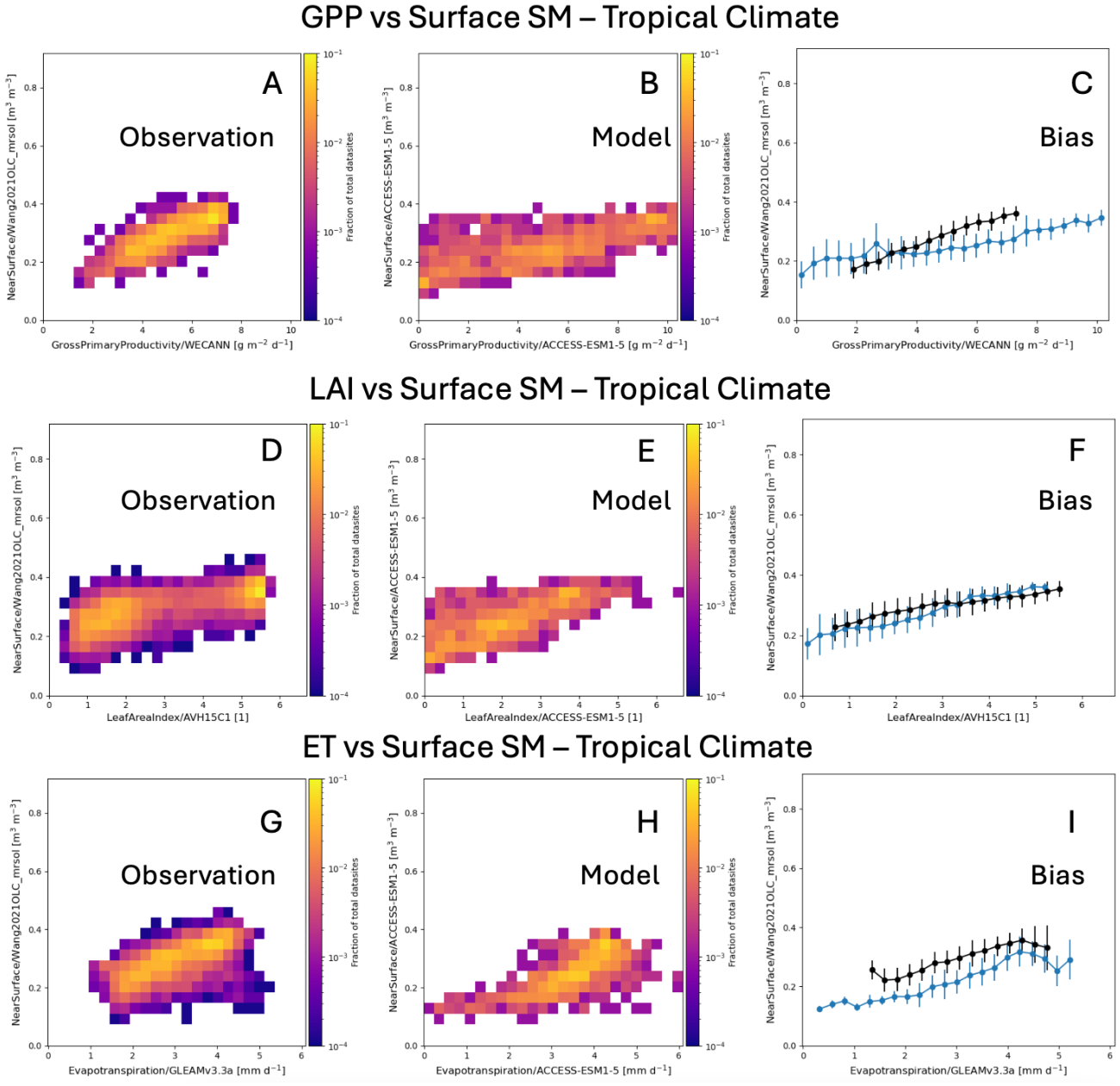

Figure A6: Relationships between surface SM and ecohydrologic variables, similar to Figure 7, but for the "Tropical" Köppen region. The model results shown here are for the ACCESS-ESM1-5 model. Panels A, D, and G show the heat maps of the observed relationships, panels B, E, and H show the heat maps of simulated relationships in the ACCESS-ESM1-5 model, and panels C, F, and I portray both the observed and simulated relationships in the form of dot and whisker plots for easy comparison.

https://doi.org/10.5194/egusphere-2025-3517
Preprint. Discussion started: 10 September 2025

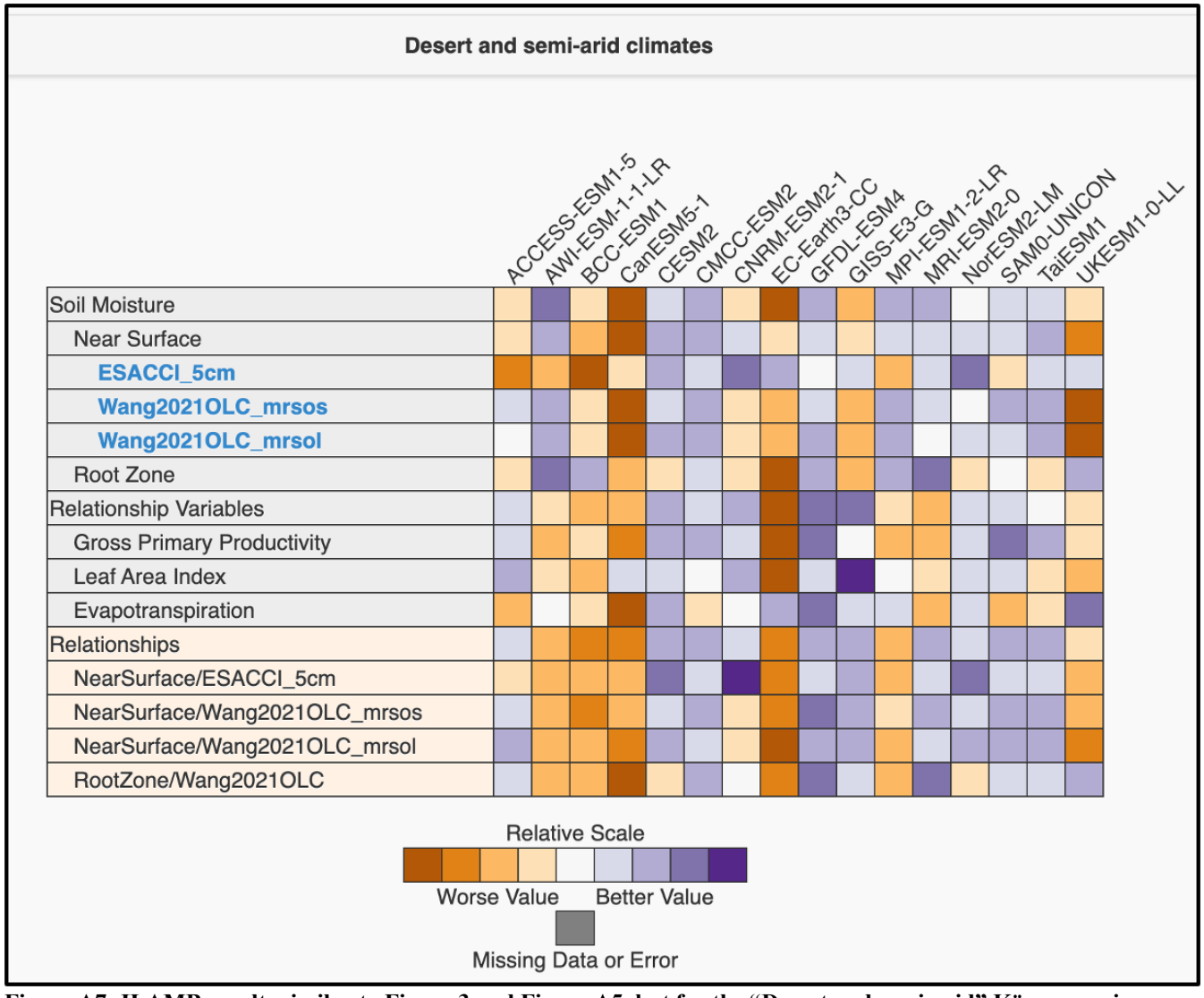

Figure A7: ILAMB results similar to Figure 3 and Figure A5, but for the "Desert and semi-arid" Köppen region.

https://doi.org/10.5194/egusphere-2025-3517
Preprint. Discussion started: 10 September 2025

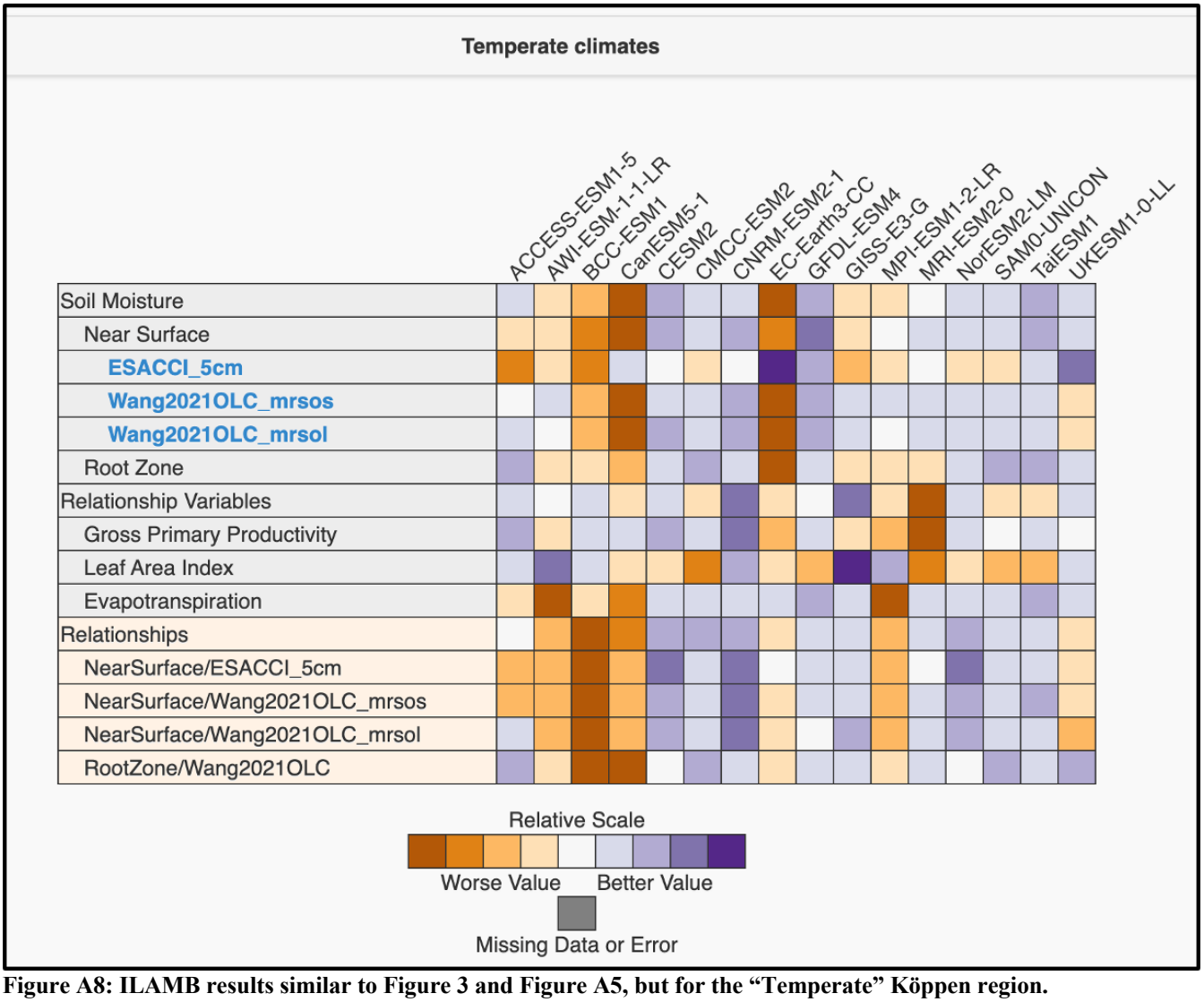

Figure A8: ILAMB results similar to Figure 3 and Figure A5, but for the "Temperate" Köppen region.

https://doi.org/10.5194/egusphere-2025-3517
Preprint. Discussion started: 10 September 2025

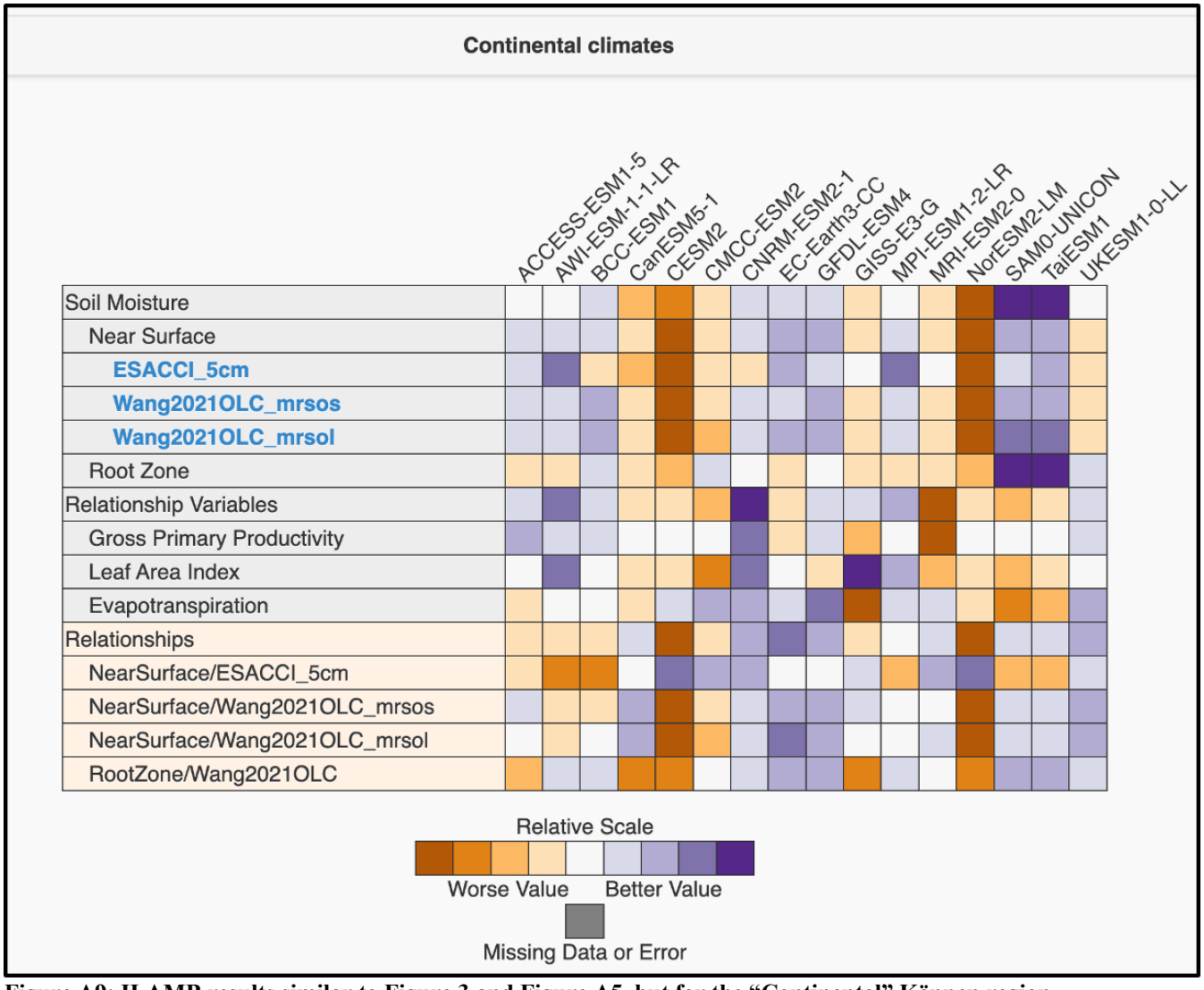

Figure A9: ILAMB results similar to Figure 3 and Figure A5, but for the "Continental" Köppen region.

https://doi.org/10.5194/egusphere-2025-3517
Preprint. Discussion started: 10 September 2025

Acknowledgements

The authors declare no conflicts of interest. This research was partially supported by the RUBISCO Science Focus Area (RUBISCO SFA KP1703), which is sponsored by the Regional and Global Model Analysis (RGMA) activity of the Earth and Environmental Systems Modeling (EESM) Program in the Earth and Environmental Systems Sciences Division (EESSD) of the Office of Biological and Environmental Research (BER) in the U.S. Department of Energy Office of Science. This work is the result of the RUBISCO project Soil Moisture Working Group effort on benchmarking soil moisture in Earth System Models, supported by the RUBISCO SFA. This paper has been authored by UT-Battelle, LLC, under contract DE-AC05-00OR22725 with the U.S. Department of Energy (DOE). P.R. acknowledges a grant from the Climate Program Office (CPO) of the National Oceanic and Atmospheric Administration (NOAA, NA22OAR4310612). The U.S. government retains and the publisher, by accepting the article for publication, acknowledges that the U.S. government retains a nonexclusive, paid-up, irrevocable, worldwide license to publish or reproduce the published form of this paper, or allow others to do so, for U.S. government purposes. DOE will provide public access to these results of federally sponsored research in accordance with the DOE Public Access Plan.

Author Contributions

This work arises from collaborative efforts and discussions within the RUBISCO Soil Moisture Working Group, which inspired the ideas behind this paper. E.C.M. performed the analysis, wrote the original draft, and led the editing process. N.C., Y.W., and J.M. helped with the analysis, contributed to discussions that shaped the paper, and assisted with editing. A.H., S.A.K., G.K., M.K., Pu.R., Pa.R., M.S., J.T., S.P.V., H.W., Q.Z., and F.M.H. contributed to the development of ideas through discussions and assisted with manuscript editing.

Code/Data Availability

The ILAMB software used in this study is publicly available at https://github.com/rubisco-sfa/ILAMB and archived with DOI: 10.18139/ILAMB.v002.00/1251621 (Collier et al., 2023). The specific assets related to the RUBISCO Soil Moisture Working Group benchmarking effort are available at https://github.com/rubisco-sfa/soil-moisture.

References

Alemohammad, S. H., Fang, B., Konings, A. G., Aires, F., Green, J. K., Kolassa, J., Miralles, D., Prigent, C., and Gentine, P. (2017). Water, Energy, and Carbon with Artificial Neural Networks (WECANN): a statistically based estimate of global surface turbulent fluxes and gross primary productivity using solar-induced fluorescence, Biogeosciences, 14, 4101–4124, https://doi.org/10.5194/bg-14-4101-2017.

https://doi.org/10.5194/egusphere-2025-3517
Preprint. Discussion started: 10 September 2025

An, R., Zhang, L., Wang, Z., Quaye-Ballard, J.A., You, J., Shen, X., Gao, W., Huang, L., Zhao, Y. and Ke, Z., 2016. Validation of the ESA CCI soil moisture product in China. International Journal of Applied Earth Observation and Geoinformation, 48, pp.28-36. https://doi.org/10.1016/j.jag.2015.09.009

Clark, M. P., Fan, Y., Lawrence, D.M., Adam, J.C., Bolster, D., Gochis, D.J., Hooper, R.P. et al. (2015). Improving the representation of hydrologic processes in Earth System Models. Water Resources Research, 51, no. 8, 5929-5956. https://doi.org/10.1002/2015WR017096

Caen, A., Smallman, T.L., de Castro, A.A., Robertson, E., von Randow, C., Cardoso, M. and Williams, M., 2022. Evaluating two land surface models for Brazil using a full carbon cycle benchmark with uncertainties. Climate Resilience and Sustainability, 1(1), p.e10. https://doi.org/10.1002/cli2.10

Claverie, M., Matthews, J., Vermote, E., and Justice, C. (2016), A 30+ Year AVHRR LAI and FAPAR Climate Data Record: Algorithm Description and Validation, Remote Sensing, 8, 263, https://doi.org/10.3390/rs8030263

Ciabatta, L., Massari, C., Brocca, L., Gruber, A., Reimer, C., Hahn, S., Paulik, C., Dorigo, W., Kidd, R., and Wagner, W., 2018: SM2RAIN-CCI: a new global long-term rainfall data set derived from ESA CCI soil moisture, Earth Syst. Sci. Data, 10, 267–280, https://doi.org/10.5194/essd-10-267-2018.

Collier, N., Hoffman, F.M., Lawrence, D.M., Keppel-Aleks, G., Koven, C.D., Riley, W.J., Mu, M. and Randerson, J.T., 2018. The International Land Model Benchmarking (ILAMB) system: design, theory, and implementation. Journal of Advances in Modeling Earth Systems, 10(11), pp.2731-2754. https://doi.org/10.1029/2018MS001354

Collier, N., Hoffman, F. M., Mu, M., Randerson, J. T., Riley, W. J., Koven, C. D., Keppel-Aleks, G., & Lawrence, D. M. (2023). International Land Model Benchmarking (ILAMB) Package (v002.00) [Computer software]. RUBISCO Science Focus Area. https://doi.org/10.18139/ILAMB.v002.00/1251621.

Dai, Y., Shangguan, W., Wei, N., Xin, Q., Yuan, H., Zhang, S., Liu, S., Lu, X., Wang, D., and Yan, F.: A review of the global soil property maps for Earth system models, SOIL, 5, 137–158, https://doi.org/10.5194/soil-5-137-2019, 2019.

Dorigo, W. A., Gruber, A., De Jeu, R. A. M., Wagner, W., Stacke, T., Loew, A., ... & Kidd, R. (2015). Evaluation of the ESA CCI soil moisture product using ground-based observations. Remote Sensing of Environment, 162, 380-395. https://doi.org/10.1016/j.rse.2014.07.023

Dorigo, W., Wagner, W., Albergel, C., Albrecht, F., Balsamo, G., Brocca, L., Chung, D., Ertl, M., Forkel, M., Gruber, A. and Haas, E., 2017. ESA CCI Soil Moisture for improved Earth system understanding: State-of-the art and future directions. Remote Sensing of Environment, 203, pp.185-215. https://doi.org/10.1016/j.rse.2017.07.001

https://doi.org/10.5194/egusphere-2025-3517
Preprint. Discussion started: 10 September 2025

Eyring, V., Bony, S., Meehl, G. A., Senior, C. A., Stevens, B., Stouffer, R. J., and Taylor, K. E.: Overview of the Coupled Model Intercomparison Project Phase 6 (CMIP6) experimental design and organization, Geosci. Model Dev., 9, 1937–1958, https://doi.org/10.5194/gmd-9-1937-2016, 2016.

Geiger, Rudolf (1954). "Klassifikation der Klimate nach W. Köppen" [Classification of climates after W. Köppen]. Landolt-Börnstein – Zahlenwerte und Funktionen aus Physik, Chemie, Astronomie, Geophysik und Technik, alte Serie. Vol. 3. Berlin: Springer. pp. 603–607.

Green, J.K., Seneviratne, S.I., Berg, A.M. et al. Large influence of soil moisture on long-term terrestrial carbon uptake. Nature 565, 476–479 (2019). https://doi.org/10.1038/s41586-018-0848-x

Gruber, A., Scanlon, T., van der Scalie, R., Wagner, W., Dorigo, W. (2019), Evolution of the ESA CCI Soil Moisture climate data records and their underlying merging methodology, Earth System Science Data, 11, 717-739, https://doi.org/10.5194/essd-11-717-2019.

Guswa, A.J., Celia, M.A. and Rodriguez-Iturbe, I., 2002. Models of soil moisture dynamics in ecohydrology: A comparative study. Water Resources Research, 38(9), pp.5-1. https://doi.org/10.1029/2001WR000826

Harpold, A. A., & Molotch, N. P. (2015). Sensitivity of soil water availability to changing snowmelt timing in the western US. Geophysical Research Letters, 42(19), 8011-8020. https://doi.org/10.1002/2015GL065855

Hauser, M., Orth, R., and Seneviratne, S. I. Role of soil moisture versus recent climate change for the 2010 heat wave in western Russia. Geophysical Research Letters 43, no. 6 (2016): 2819-2826. https://doi.org/10.1002/2016GL068036

Hengl, T., De Jesus, J.M., MacMillan, R.A., Batjes, N.H., Heuvelink, G.B., Ribeiro, E., Samuel-Rosa, A., Kempen, B., Leenaars, J.G., Walsh, M.G. and Gonzalez, M.R., 2014. SoilGrids1km—global soil information based on automated mapping. PloS one, 9(8), p.e105992. https://doi.org/10.1371/journal.pone.0105992

Humphrey, V., Berg, A., Ciais, P. et al. Soil moisture–atmosphere feedback dominates land carbon uptake variability. Nature, 592, 65–69 (2021). https://doi.org/10.1038/s41586-021-03325-5

Lawrence, D. M., Fisher, R. A., Koven, C. D., Oleson, K. W., Swenson, S. C., Bonan, G., ... & Zeng, X. (2019). The Community Land Model version 5: Description of new features, benchmarking, and impact of forcing uncertainty. Journal of Advances in Modeling Earth Systems, 11(12), 4245-4287. https://doi.org/10.1029/2018MS001583

https://doi.org/10.5194/egusphere-2025-3517
Preprint. Discussion started: 10 September 2025

Levine, P. A., Randerson, J. T., Swenson, S. C., and Lawrence, D. M., 2016. Evaluating the strength of the land–atmosphere moisture feedback in Earth system models using satellite observations, Hydrol. Earth Syst. Sci., 20, 4837–4856, https://doi.org/10.5194/hess-20-4837-2016

Li, L., Lin, X., Fang, Y. et al. A unified ensemble soil moisture dataset across the continental United States. Sci Data, 12, 546 (2025a). https://doi.org/10.1038/s41597-025-04657-x

Li, W., Migliavacca, M., Miralles, D.G., Reichstein, M., Anderegg, W.R., Yang, H. and Orth, R. Disentangling Effects of Vegetation Structure and Physiology on Land–Atmosphere Coupling. Global Change Biology, 31(1), p.e70035. (2025b). https://doi.org/10.1111/gcb.70035

Lu, X., Du, Z., Huang, Y., Lawrence, D., Kluzek, E., Collier, N., Lombardozzi, D., Sobhani, N., Schuur, E.A. and Luo, Y., 2020. Full implementation of matrix approach to biogeochemistry module of CLM5. Journal of Advances in Modeling Earth Systems, 12(11), p.e2020MS002105. https://doi.org/10.1029/2020MS002105

Martens, B., Miralles, D. G., Lievens, H., van der Schalie, R., de Jeu, R. A. M., Fernández-Prieto, D., Beck, H. E., Dorigo, W. A., and Verhoest, N. E. C., 2017: GLEAM v3: satellite-based land evaporation and root-zone soil moisture, Geosci. Model Dev., 10, 1903–1925, https://doi.org/10.5194/gmd-10-1903-2017

Massoud, E. C., Xu, C., Fisher, R. A., Knox, R. G., Walker, A. P., Serbin, S. P., Christoffersen, B. O., Holm, J. A., Kueppers, L. M., Ricciuto, D. M., Wei, L., Johnson, D. J., Chambers, J. Q., Koven, C. D., McDowell, N. G., and Vrugt, J. A.: Identification of key parameters controlling demographically structured vegetation dynamics in a land surface model: CLM4.5(FATES), Geosci. Model Dev., 12, 4133–4164, https://doi.org/10.5194/gmd-12-4133-2019, 2019.

Massoud, E., Turmon, M., Reager, J., Hobbs, J., Liu, Z. and David, C.H., 2020. Cascading dynamics of the hydrologic cycle in California explored through observations and model simulations. Geosciences, 10(2), p.71. https://doi.org/10.3390/geosciences10020071

Massoud, E. C., Andrews, L., Reichle, R., Molod, A., Park, J., Ruehr, S., and Girotto, M.: Seasonal forecasting skill for the High Mountain Asia region in the Goddard Earth Observing System, Earth Syst. Dynam., 14, 147–171, https://doi.org/10.5194/esd-14-147-2023, 2023.

Massoud, E.C., Collier, N.O., M. Xu, M. Shi, Hoffman, F.M. 2025. Discrepancies in the representation of surface and layered soil moisture in Earth System Models. Geophysical Research Letters. Submitted. 2025.

McNally, A., Shukla, S., Arsenault, K.R., Wang, S., Peters-Lidard, C.D. and Verdin, J.P., 2016. Evaluating ESA CCI soil moisture in East Africa. International Journal of Applied Earth Observation and Geoinformation, 48, pp.96-109. https://doi.org/10.1016/j.jag.2016.01.001

https://doi.org/10.5194/egusphere-2025-3517
Preprint. Discussion started: 10 September 2025

Miralles, D. G., Holmes, T. R. H., De Jeu, R. A. M., Gash, J. H., Meesters, A. G. C. A., and Dolman, A. J.: Global land-surface evaporation estimated from satellite-based observations, Hydrol. Earth Syst. Sci., 15, 453–469, https://doi.org/10.5194/hess-15-453-2011, 2011.

Nachtergaele, F., van Velthuizen, H., Verelst, L., Wiberg, D., Henry, M., Chiozza, F., Yigini, Y., Aksoy, E., Batjes, N., Boateng, E. and Fisher, G., 2023. Harmonized world soil database version 2.0. FAO.

Oleson, K. W., Lawrence, D. M., Bonan, G. B., Fisher, R. A., Lawrence, P. J., & Muszala, S. P. (2013). Technical description of version 4.5 of the Community Land Model (CLM). Technical description of version 4.5 of the Community Land Model (CLM)(2013) NCAR/TN-503+ STR, 503. DOI: 10.5065/D6RR1W7M

Preimesberger, W., Scanlon, T., Su, C. -H., Gruber, A. and Dorigo, W. (2021). Homogenization of Structural Breaks in the Global ESA CCI Soil Moisture Multisatellite Climate Data Record, in IEEE Transactions on Geoscience and Remote Sensing, vol. 59, no. 4, pp. 2845-2862, April 2021, doi: 10.1109/TGRS.2020.3012896.

Preimesberger, W., Stradiotti, P., and Dorigo, W.: ESA CCI Soil Moisture GAPFILLED: An independent global gap-free satellite climate data record with uncertainty estimates, Earth Syst. Sci. Data Discuss. [preprint], https://doi.org/10.5194/essd-2024-610, in review, 2025.

Purdy, A. J., Fisher, J. B., Goulden, M. L., Colliander, A., Halverson, G., Tu, K., & Famiglietti, J. S. (2018). SMAP soil moisture improves global evapotranspiration. Remote Sensing of Environment, 219, 1-14. https://doi.org/10.1016/j.rse.2018.09.023

Qiao, L., Zuo, Z., and Xiao, D. "Evaluation of soil moisture in CMIP6 simulations." Journal of Climate 35, no. 2 (2022): 779-800. https://doi.org/10.1175/JCLI-D-20-0827.1

Robock, A., Schlosser, C.A., Vinnikov, K.Y., Speranskaya, N.A., Entin, J.K. and Qiu, S., 1998. Evaluation of the AMIP soil moisture simulations. Global and Planetary Change, 19(1-4), pp.181-208. https://doi.org/10.1016/S0921-8181(98)00047-2

Seneviratne, S. I., Corti, T., Davin, E. L., Hirschi, M., Jaeger, E. B., Lehner, I., Orlowsky, B., and Teuling, A. J.. "Investigating soil moisture–climate interactions in a changing climate: A review." Earth-Science Reviews 99, no. 3-4 (2010): 125-161. https://doi.org/10.1016/j.earscirev.2010.02.004

Shangguan, W., Dai, Y., Duan, Q., Liu, B. and Yuan, H., 2014. A global soil data set for earth system modeling. Journal of Advances in Modeling Earth Systems, 6(1), pp.249-263. https://doi.org/10.1002/2013MS000293

https://doi.org/10.5194/egusphere-2025-3517
Preprint. Discussion started: 10 September 2025

Schumacher, D.L., Keune, J., Dirmeyer, P. et al. Drought self-propagation in drylands due to land–atmosphere feedbacks. Nat. Geosci. 15, 262–268 (2022). https://doi.org/10.1038/s41561-022-00912-7

Talib, J., Müller, O.V., Barton, E.J. et al. The Representation of Soil Moisture-Atmosphere Feedbacks across the Tibetan Plateau in CMIP6. Adv. Atmos. Sci. 40, 2063–2081 (2023). https://doi.org/10.1007/s00376-023-2296-2

Tapiador, F.J., Navarro, A., Jiménez, A., Moreno, R. and García-Ortega, E., 2018. Discrepancies with satellite observations in the spatial structure of global precipitation as derived from global climate models. Quarterly Journal of the Royal Meteorological Society, 144, pp.419-435. https://doi.org/10.1002/qj.3289

Trugman, A. T., D. Medvigy, J. S. Mankin, and W. R. L. Anderegg. "Soil moisture stress as a major driver of carbon cycle uncertainty." Geophysical Research Letters 45, no. 13 (2018): 6495-6503. https://doi.org/10.1029/2018GL078131

Vogel, M. M., Zscheischler, J., and Seneviratne, S. I.: Varying soil moisture–atmosphere feedbacks explain divergent temperature extremes and precipitation projections in central Europe, Earth Syst. Dynam., 9, 1107–1125, https://doi.org/10.5194/esd-9-1107-2018, 2018.

Wang, C., Fu, B., Zhang, L. and Xu, Z., 2019. Soil moisture–plant interactions: an ecohydrological review. Journal of Soils and Sediments, 19, pp.1-9. https://doi.org/10.1007/s11368-018-2167-0

Wang, Y., Mao, J., Jin, M., Hoffman, F. M., Shi, X., Wullschleger, S. D., and Dai, Y.: Development of observation-based global multilayer soil moisture products for 1970 to 2016, Earth Syst. Sci. Data, 13, 4385–4405, https://doi.org/10.5194/essd-13-4385-2021, 2021.

Wang, A., Kong, X., Chen, Y., & Ma, X. (2022). Evaluation of soil moisture in CMIP6 multi model simulations over conterminous China. Journal of Geophysical Research: Atmospheres,127, e2022JD037072. https://doi.org/10.1029/2022JD037072

Wu, G., Cai, X., Keenan, T.F., Li, S., Luo, X., Fisher, J.B., Cao, R., Li, F., Purdy, A.J., Zhao, W. and Sun, X., 2020. Evaluating three evapotranspiration estimates from model of different complexity over China using the ILAMB benchmarking system. Journal of Hydrology, 590, p.125553. https://doi.org/10.1016/j.jhydrol.2020.125553

Yamaguchi, M., Lang, S.T., Leutbecher, M., Rodwell, M.J., Radnoti, G. and Bormann, N., 2016. Observation-based evaluation of ensemble reliability. Quarterly Journal of the Royal Meteorological Society, 142(694), pp.506-514. https://doi.org/10.1002/qj.2675

Yang, X., Thornton, P., Ricciuto, D., Wang, Y., and Hoffman, F.: Global evaluation of terrestrial biogeochemistry in the Energy Exascale Earth System Model (E3SM) and the role of the phosphorus

https://doi.org/10.5194/egusphere-2025-3517
Preprint. Discussion started: 10 September 2025

cycle in the historical terrestrial carbon balance, Biogeosciences, 20, 2813–2836, https://doi.org/10.5194/bg-20-2813-2023, 2023.

Yuan, S., Quiring, S. M., & Leasor, Z. T. (2021). Historical changes in surface soil moisture over the contiguous United States: An assessment of CMIP6. Geophysical Research Letters, 48(1), e2020GL089991. https://doi.org/10.1029/2020GL089991

Zeng, J., Peng, J., Zhao, W., Ma, C., & Ma, H. (2023). Microwave remote sensing of soil moisture. Remote Sensing, 15(17), 4243. https://doi.org/10.3390/rs15174243

Zuo, Z., Qiao, L., Zhang, R., Chen, D., Piao, S., Xiao, D., & Zhang, K. (2024). Importance of soil moisture conservation in mitigating climate change. Science Bulletin, 69(9), 1332-1341. https://doi.org/10.1016/j.scib.2024.02.033